CHAPTER 5

EPR Spin Trapping

5.1 INTRODUCTION

There has never been a more desirable way to detect radicals than by direct detection, and this can be achieved through the use of electron paramagnetic resonance (EPR) spectroscopy. Although it is possible to directly detect free radicals alone, the single most important limitation for detecting them is their extremely short half-life in aqueous solution. For example, although $O_2^{\bullet -}$ is a weak base (pK_a of its conjugate acid = 4.69), it can abstract protons from water, according to the Eq. (5.1), with an equilibrium constant of $K_{eq} = 0.9 \times 10^9$, thus favoring its almost instantaneous decay to the diamagnetic products.[1]

$$2O_2^{\bullet -} + H_2O \rightleftharpoons HO_2^- + O_2 + HO^- \tag{5.1}$$

Direct detection of $HO^{\bullet}$ itself in solution is even more difficult due to its high bimolecular reaction with $k_2 = 0.5 \times 10^{10}\ M^{-1}\,s^{-1}$, according to Eq. (5.2).[2]

$$2HO^{\bullet} \rightarrow H_2O_2 \tag{5.2}$$

The favorability of radicals to decompose in aqueous solution translates to short lifetimes; in the presence of biological milieu, their lifetimes are expected to be even shorter.

In the case of $O_2^{\bullet -}$, its direct detection by EPR spectroscopy was achieved in glassy protic and aprotic solvents through rapid freezing techniques at temperatures in the range of 4–280K.[3–6] Direct $O_2^{\bullet -}$ detection was also accomplished in the presence of colloidal TiO_2 at room temperature[7] as well in the presence of Ti^{3+} and ionomeric polymers in the temperature range of 220–320K.[8]

Fig. 5.1 shows the EPR spectra of $O_2^{\bullet -}$ from the electrochemical reduction of oxygen in butyronitrile at various temperatures.[3] While it is possible to detect free radicals alone in solution, it requires special solvents and stabilizing agents such as metal ions, so this means limiting the application of radical detection in biological systems at ambient conditions. Since cellular organization, cell viability, energy utilization, chemical and biomechanical activities, enzymatic function, metabolic regulation, and cell structural integrity all depend on temperature and microenvironment conditions, it is desirable to detect radicals at the site of their formation—i.e., from their native source and in normal conditions. Direct radical detection in biology faces difficult technical challenges

Reactive Species Detection in Biology
DOI: http://dx.doi.org/10.1016/B978-0-12-420017-3.00004-9

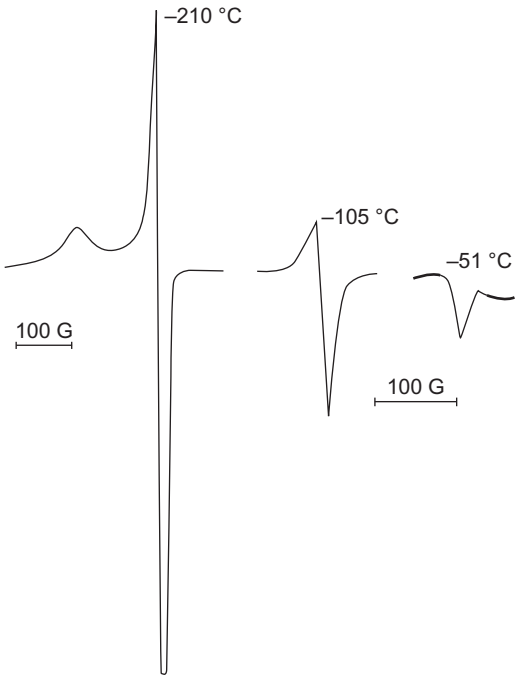

Figure 5.1 Anisotropic EPR spectra of $O_2^{\bullet -}$ in the liquid phase from electrochemical reduction of molecular oxygen with $g_{\parallel} = 2.072$ and $g_{\perp} = 2.009$.[3] *Reprinted with permission from Bagchi et al. Characterization of the ESR spectrum of the superoxide anion in the liquid phase. J Am Chem Soc 1989;**111**:8270–1. Copyright © 1989 American Chemical Society.*

since radicals are mostly produced at ambient conditions; freezing the cells or tissue will inhibit radical formation. Although there is a basal radical generation in cells in the absence of external stimuli, their concentrations are too low to be detected by EPR spectroscopy, which brings us to another technical aspect in radical detection in biological systems because most radicals are produced from the oxidative burst generated from the stimulation of enzymes or cells by external stimulants. Radicals are generated almost instantaneously with the introduction of exogenous agents, so timing is critical when it is desirable to detect radicals in situ immediately after stimulation. When radical initiators are added, users only have a few seconds to place the sample in the EPR cavity, and a few more precious seconds are lost during the initial acquisitions.

The mode by which radical initiators are added into the solution has been a challenge, and stopped-flow EPR techniques have been developed at time resolutions of seconds to minutes,[9] but those with millisecond time resolution require a much more specialized loop-gap resonator technology[10] and were found to be useful for investigating the kinetics of radical production in various biological systems. Although stopped-flow EPR seems useful for the direct detection of transient radicals, their

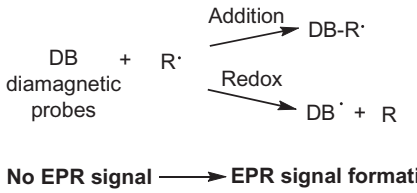

Scheme 5.1 Routes of diamagnetic probe to paramagnetic probe formation.

time resolution is still not short enough to detect short-lived radicals such as $O_2^{\bullet -}$ and $HO^{\bullet}$ in solution due to their very short half-lives, which range from a nanosecond to a microsecond. Hence, the use of diamagnetic or paramagnetic probes to "stabilize" or "probe" these radicals has become essential for the detection of short-lived radicals in solution. Since probes are reagents used to detect radicals, technically one could not claim such a technique to be direct radical detection anymore since the reaction between the probe and the radical is the one that is being monitored by EPR and not the radicals directly themselves.

Probes could be broadly defined as reagents that are employed to qualitatively and quantitatively measure radical species. Probes could be categorized into two main classes: (1) diamagnetic and (2) paramagnetic. Two commonly used diamagnetic probes are nitrone and hydroxylamine, and both impart EPR signals by spin formation after addition or redox reaction with the radical species, respectively, as shown in Scheme 5.1:

The development of small molecule probes, both diamagnetic and paramagnetic, paved the way for a more convenient measurement of free radical formation under normal conditions. The most commonly used diamagnetic probe to date are the nitrone based (commonly referred to as *spin traps*) and the hydroxylamines, while the paramagnetic ones are stable radicals such as nitroxides and trityl radicals. Due to the ability of the EPR spectrum of the probes to be formed, quenched, or transformed in the presence of radicals, the EPR technique is a powerful tool that can provide key information on the following and even more: (1) concentration of reactive species formed, (2) nature of the radical formed, (3) kinetics of radical formation, and (4) oxygen concentration. Therefore, the biomedical values of spin trapping include understanding the origins of radical production, the toxicology of xenobiotics, and the antioxidant activities of some compounds as well as improving the accuracy of radical identification from the cellular level to whole animals using EPR spectroscopy.

5.2 ELECTRON PARAMAGNETIC RESONANCE SPECTROSCOPY

Electron paramagnetic resonance (EPR) or electron spin resonance (ESR) spectroscopy is a magnetic resonance technique commonly used in the detection of paramagnetic species.[11] This involves absorption of microwave radiation by the unpaired electron in

the presence of an external magnetic field, resulting in the transition between two spin states. The energy absorbed corresponds to the energy of splitting between the two spin states and is directly proportional to the applied magnetic field strength commonly called the *Zeeman effect* and is described by the fundamental Eq. (5.3):

$$\Delta E = h\nu = g\Delta H \tag{5.3}$$

where ΔE corresponds to the energy of absorbed microwave energy, h is Planck's constant, ν is the frequency of applied electromagnetic radiation, g is a factor equal to 2.0023 for a free electron, and H is the applied field strength. Any species bearing an unpaired electron such as a free radical, transition metals, or biradicals with triplet ground states are typically detectable by EPR using conventional x-band spectrometer at ~9.8 GHz microwave frequency, which is generated by a solid-state Gunn diode. The sample is placed in the cavity between the poles of two magnets and in the presence of microwave radiation. Typically, microwave absorption by the sample is measured by increasing the magnetic-field strength at constant frequency, and the spectrum is presented as a first-derivative spectrum for improved sensitivity. However, detection of radicals in biological systems is often limited by their short half-lives and, therefore EPR techniques that use spin traps and redox probes that yield (or quench) persistent or stable radicals are desirable.

5.3 CHEMISTRY OF SPIN TRAPPING

Spin trapping is an analytical technique employed to detect and identify transient free radicals, although this is not limited to radical species because nitrones are susceptible to nucleophilic addition reactions as well, which will be discussed in the succeeding section. Nitrone is a functionality that is chemically similar in reactivity to carbonyl compounds such as ketones and aldehydes. The carbon doubly bonded to the nitrogen called nitronyl-carbon has significant positivity that it is susceptible to nucleophilic addition reaction, which is analogous to the carbonyl-carbons.

	Nitrone	Carbonyl
	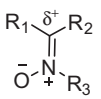	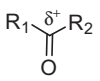
$R_1 = R_2$ = alkyl	Ketonitrone	Ketone
R_1 = alkyl; R_2 = H	Aldonitrone	Aldehyde

But what makes nitrones uniquely different from carbonyl compounds is their ability to undergo addition reaction with radical species to form a more persistent

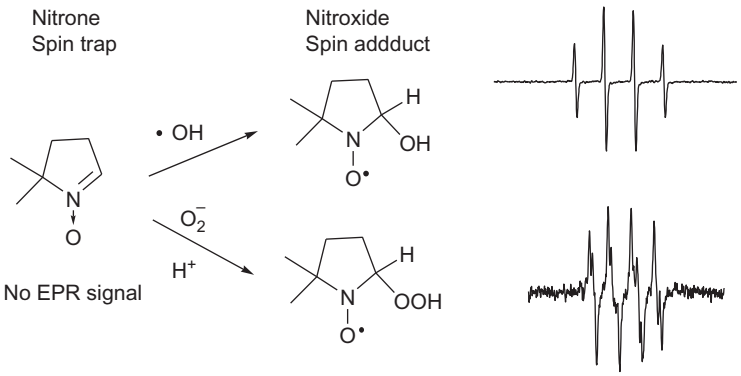

Figure 5.2 EPR signals from spin or radical adduct formation.

nitroxide radical (Eq. 5.4). Since the radical species being trapped contain an unpaired electron with an intrinsic spin, nitrones are usually referred to as *spin trap* and the nitroxide as a *spin adduct*.

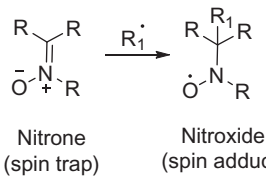

(5.4)

Spin trapping is one of the very few analytical techniques that can identify the nature or structure of a radical intermediate. The EPR signal that is produced by the nitroxide spin adduct provides a wealth of information due to their ability to not only *quantify* the amount of radicals produced but also to identify radicals rather than just detect them, which is one unique feature of spin trapping over the use of other techniques. The most attractive feature of the spin-trapping technique is its ability to discern various radicals formed from each other based on their spectral profiles (e.g., hyperfine splitting constants, line width, or symmetry) of their spin adduct. For example, in Fig. 5.2, two different EPR spectral profiles can be seen from the addition of $O_2^{\bullet -}$ or $HO^{\bullet}$ to the spin trap, 5,5-dimethylpyrroline-*N*-oxide (DMPO). Therefore, with spin trapping, one could differentiate O-centered radicals such as $O_2^{\bullet -}$, $HO^{\bullet}$, and $RO^{\bullet}$ as well as C, N, and S radicals from each other and is typically referred to as *spectral fingerprinting*, which is similar in concept to ^1H—nuclear magnetic resonance and infrared spectroscopic techniques.

5.4 CLASSIFICATION OF SPIN TRAPS

Two major classes of spin traps are commonly employed in spin trapping: (1) cyclic and (2) linear nitrones as shown in Fig. 5.3. The most common cyclic nitrone is the 5,5-

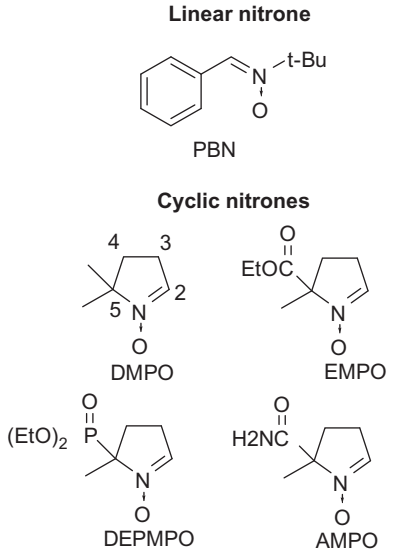

Figure 5.3 Common types of nitrone spin traps.

dimethylpyrroline-*N*-oxide (DMPO), while for the linear one it is *N*-tert-butyl-α-phenyl nitrone (PBN). A number of cyclic spin traps have been synthesized over the past years (e.g., imidazole,[12,13] isoindole,[14] indole-one[15] nitrones), but they do not trap $O_2^{\bullet-}$. In the case of trifluoromethyl-pyrroline,[16] isoquinoline, and benzazepine[17] nitrones, the resulting $O_2^{\bullet-}$ adducts have short half-lives. Moreover, bicyclic nitrones exhibited a very complex spectrum.[18,19] Most PBN-type nitrones are mostly limited by their inability to trap $O_2^{\bullet-}$, but even if they do the adducts are too unstable to be detectable by EPR.[17] Although the possibility for designing new nitrones seems endless, hurdles are typically encountered in the application of new nitrones in biological systems.

To date, only DMPO-type nitrones exhibit the most promising spin-trapping properties compared to any nitrone-based spin traps. This is due to their low cytoxicity, faster reactivity to $O_2^{\bullet-}$ compared to PBN-type nitrones,[20] longer half-lives of the respective $O_2^{\bullet-}$ adducts, and their ability to give distinguishable EPR spectrum on reaction with radicals, specifically those of O-centered radicals due to the conformational rigidity of the pyrroline-ring system, which is perhaps the most important feature of such class of compounds. To improve DMPO spin-trapping properties, its derivatization at the C-5 position with alkoxyphosphoryl, alkoxycarbonyl, or carbamoyl (Fig. 5.3) as exemplified by 5-(diethoxyphosphoryl)-5-methyl-1-pyrroline *N*-oxide (DEPMPO),[21] 5-ethoxycarbonyl-5-methyl-1-pyrroline-*N*-oxide (EMPO),[22] and 5-carbamoyl-5-methyl-1-pyrroline-*N*-oxide (AMPO),[23] respectively, gave longer half-lives for their respective $O_2^{\bullet-}$ adducts or improved reactivities to $O_2^{\bullet-}$ or both. However, 5-substituted nitrones still suffer certain limitations as will be discussed in the succeeding section.

5.5 KINETICS AND THERMODYNAMICS OF SPIN TRAPPING AND pH EFFECT

Two important kinetic properties have to be considered in employing spin traps for radical detection—i.e., the kinetics of spin trapping and adduct decay. While nitric oxide (NO) is unreactive toward DMPO, the reported experimental apparent rate constant for the reaction of DMPO with $O_2^{\bullet-}$ is $1-170\ M^{-1}s^{-1}$,[24,25] $600\ M^{-1}s^{-1}$ with $HO_2^{\bullet}$,[26] $1.1\times10^6\ M^{-1}s^{-1}$ with $CH_3^{\bullet}CHOH$,[27] $1.1\times10^6\ M^{-1}s^{-1}$ with glutathiyl radical $GS^{\bullet}$,[28] and $1.93\times10^9\ M^{-1}s^{-1}$ with $HO^{\bullet}$.[29] This shows that the order of increasing rate of addition of radicals to DMPO is $NO < O_2^{\bullet-} < HO_2^{\bullet} < CH_3^{\bullet}CHOH < GS^{\bullet} < HO^{\bullet}$. These kinetics of radical addition to DMPO correlate well with the reduction potentials of the respective radicals showing the same order of increasing oxidizing capability (reported as $E^{\circ\prime}$ values, V): $NO < (-0.80) < HS^{\bullet}$ or $GS^{\bullet}$ (0.92)[31] $< O_2^{\bullet-}$ $(0.94) < HO_2^{\bullet}$ $(1.06) < {}^{\bullet}CH_3$ $(1.90) < HO^{\bullet}$ (2.31),[30,31] with the exception of the thiyl radicals. However, the calculated free energies of reaction (ΔG_{rxn}, kcal/mol) in aqueous phase of various radicals to DMPO at the PCM/B3LYP/6-31 + G(d,p)//B3LYP/6-31G(d) level gave the following order of increasing favorability: $NO < (15.1) < O_2^{\bullet-}$ $(3.4) < HO_2^{\bullet}$ $(-12.8) < HS^{\bullet}$ $(-15.5) < {}^{\bullet}CH_3$ $(-30.2) < HO^{\bullet}$ (-42.1).[32] The calculated average free energies of reaction (ΔG_{rxn}, kcal/mol) from 10 different spin traps with various radicals according to increasing favorability is $NO < (14.6) < O_2^{\bullet-}$ $(-7.5) < HO_2^{\bullet}$ $(-13.9) < HS^{\bullet}$ $(-16.6) < {}^{\bullet}CH_3$ $(-32.2) < HO^{\bullet}$ (-43.7).[32] Regardless of the spin trap being used, thiyl, carbon-centered radical and hydroxyl radicals always exhibit the highest favorability and rates of reaction to nitrones and therefore would be the easiest to detect in solution using the minimal concentrations typically used for spin trapping ($\sim$0.1–1 mM). However, with $O_2^{\bullet-}$ and $HO_2^{\bullet}$—whose reactivities are orders of magnitude less favorable compared to thiyl—carbon-centered radical and hydroxyl radicals would require higher concentrations of the spin traps in the range of 10–100 mM.

Based on the kinetic and thermodynamic data of spin trapping, the detection of $O_2^{\bullet-}$ or $HO_2^{\bullet}$ or both are the two most challenging due to their low reactivities compared to other radicals. However, in spin trapping, it is the $HO_2^{\bullet}$ adduct that is detected, even if the $O_2^{\bullet-}$ was initially trapped. There are three conditions by which $HO_2^{\bullet}$ adduct could be formed, depending on the pH of the solution: (1) at pH above the pK_a of the conjugate acid (i.e., $HO_2^{\bullet}$) of $O_2^{\bullet-}$; (2) at pH below the pK_a of the nitrone–H^+; and (3) at pH below the pK_a of $HO_2^{\bullet}$. The pK_a of $HO_2^{\bullet}$ was experimentally determined to be 4.8[33] (or 4.4)[34] as shown in Eq. (5.5)

$$HO_2^{\bullet} \overset{pK_a = 4.8}{\rightleftharpoons} O_2^{\bullet-} + H^+ \tag{5.5}$$

And therefore at pH > 4.8, the spin trapping of $O_2^{\bullet -}$ predominates, according to Eq. (5.6), which shows the calculated free energies:

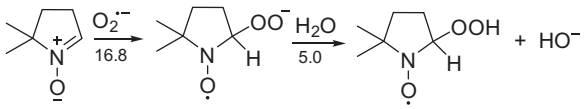

(5.6)

The high positive $\Delta G_{rxn,aq}$ of 16.8 kcal/mol for the addition of $O_2^{\bullet -}$ to DMPO is reflected in its low rate of reaction with $k = 2\ M^{-1}\,s^{-1}$.[35]

A second scenario is spin trapping at pH below the pK_a of the nitrone−H^+. Because the pK_a of the conjugate acid of DMPO was determined to be 6.0,[36] the protonation of DMPO would be more favored than the protonation of $O_2^{\bullet -}$ at slightly acidic pH, according to Eq. (5.7):

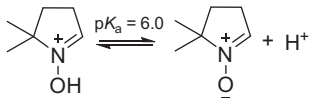

(5.7)

This could lead to higher favorability of $O_2^{\bullet -}$ addition to DMPO−H^+ due to a higher

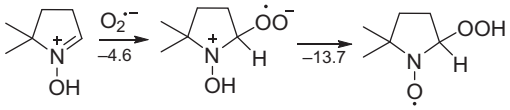

(5.8)

partial positive character on the nitronyl-C, making it more susceptible to nucleophilic addition reactions, similar to those observed for the enhanced nucleophilic addition reaction of carbonyl compounds under acidic condition. This is evidenced by the exoergic free energy of reaction of $O_2^{\bullet -}$ to DMPO−H^+ of −4.6 kcal/mol (Eq. 5.8) and subsequent intramolecular proton transfer with free energy of reaction of −13.7 kcal/mol.[36] This translates to a higher experimental rate constant of $k \sim 27\ M^{-1}\,s^{-1}$ for the spin trapping of DMPO at pH 6.2 which was found to be higher compared to that in pH 7.2 with $k \sim 2\ M^{-1}\,s^{-1}$ or pH 9.3 with $k \sim 0.35\ M^{-1}\,s^{-1}$.[26]

Spin trapping below the pK_a of $HO_2^{\bullet}$ of 4.8 offers another possibility of adduct formation via direct addition of $HO_2^{\bullet}$ to the nitrone. Since $HO_2^{\bullet}$ is a stronger oxidizer than $O_2^{\bullet -}$, it is expected that this reaction would impart a higher rate of reaction as well as favorability, according to Eq. (5.9),

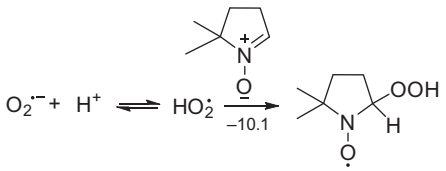

(5.9)

with an exoergic free energy of reaction of $\Delta G_{rxn,aq} = -10.1$ kcal/mol. The experimental rate constants for $O_2^{\bullet -}$ addition to DMPO were reported to be 10 $M^{-1}s^{-1}$ at pH 7 and 6600 $M^{-1}s^{-1}$ at pH 5.[37] In summary, solution pH affects the rate of $O_2^{\bullet -}$ trapping. As shown in Fig. 5.4, the pH dependence of apparent rate constant of spin trapping of $O_2^{\bullet -}$ by DMPO follows an inverse correlation in which the spin trapping is faster in acidic conditions compared to basic solutions.[37]

Aside from the solution pH, the rate of $O_2^{\bullet -}$ trapping is also affected by several factors, depending on the type of (1) radical generating system, (2) spin trap, (3) solvent system, and (4) kinetic model used in the calculation. Table 5.1 is a compilation of the various apparent rate constants for the $O_2^{\bullet -}$ trapping by DMPO, DEPMPO, 5-butoxycarbonyl-5-methyl-1-pyrroline-*N*-oxide (BMPO), EMPO, and 5,5-diethoxycarbonyl-1-pyrroline-*N*-oxide (DEPO). For example, using DMPO, rate constants can range from 2 to 170 $M^{-1}s^{-1}$, and no general trend in rate constant can be seen across all the spin-trapping agents used, which indicates that it is very important to use DMPO or DEPMPO as the gold standard for rate measurements when determining rate constants for newly developed spin traps.

What is clear, however, is that DFT studies reveal the direct proportionality of the charge density on the nitronyl-carbon to the favorability and rate of $O_2^{\bullet -}$ reaction to nitrones as shown in Fig. 5.5. Computational study shows that electron-withdrawing substituents such as *N*-monoalkylsubstituted amide or an ester as substituent at the C-5 position of the nitrone gave improved favorability and rate of spin-trapping properties, further demonstrating the nucleophilic nature of $O_2^{\bullet -}$. The synthesis of AMPO provided two important insights into the factors that govern high reactivity of $O_2^{\bullet -}$ to nitrones (Fig. 5.6): (1) increased electrophilicity of C-2 (the site of $O_2^{\bullet -}$ addition)

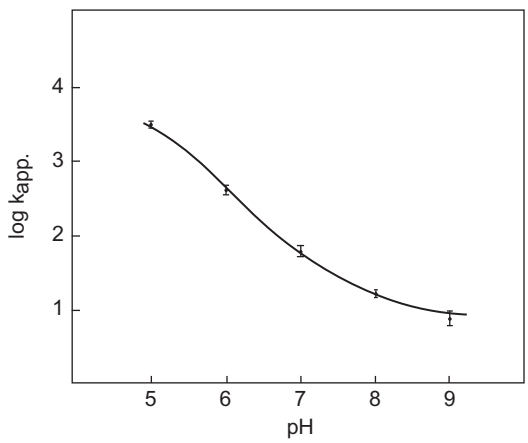

Figure 5.4 Effect of pH on the apparent rate constant for the trapping of $O_2^{\bullet -}/HO_2^{\bullet}$ by DMPO using a light-riboflavin superoxide generating system. The solid line yields rate constants of $k_{HO2} = 6.6 \times 10^3\ M^{-1}s^{-1}$ and $k_{O2} = 10\ M^{-1}s^{-1}$. *Reprinted with permission from Finkelstein et al. Spin trapping. Kinetics of the reaction of superoxide and hydroxyl radicals with nitrones. JACS 1980;**102**:4994–9. Copyright © 1980 American Chemical Society.*

Table 5.1 Survey of the reported apparent rate constants k_{app} ($M^{-1}\,s^{-1}$) for the spin trapping of superoxide radical by DMPO-type nitrones using various methodologies (technique used, competitor, radical generating system and pH)[24]

Method	Rate constants k_{app} ($M^{-1}\,s^{-1}$)				
	DMPO	DEPMPO	BMPO[a]	EMPO	DEPO
I.[38] EPR, superoxide dismutase (SOD), light-riboflavin, pH 7.0	N/A[b]	58	7	N/A	N/A
II.[37] EPR, SOD, light-riboflavin, pH 8.0	15.7	N/A	N/A	N/A	N/A
III.[21,39] EPR, light-riboflavin, pH 7.0	N/A	90c	N/A	N/A	N/A
IV.[40–42] EPR, $O_2^{\bullet-}$ dismutation X/XO, 7.2	2.0	3.95	3.45	10.9	31.1
V.[43] EPR, ferricytochrome-c, X/XO, 7.0	78.5 ± 2.1	N/A	77.0 ± 5.0	74.5 ± 6.4	N/A
VI.[44] EPR, $O_2^{\bullet-}$ dismutation, X/XO, 7.4	2.4	0.53	0.24	N/A	N/A
VII.[45] Pulse radiolysis, γ-irradiation of N_2O	170 ± 40	N/A	< 3	N/A	N/A
VIII[24] UV visible (UV vis), stopped-flow, phenol red, KO_2, pH 10.5	1.72 ± 0.01	0.65 ± 0.01	N/A	104.6 ± 4.6	N/A
IX[25] EPR, $O_2^{\bullet-}$ dismutation, X/XO, 7.4	30	N/A	N/A	N/A	N/A
X[46] EPR, nicotinamide adenine dinucleotide phosphate (NADPH)−cytochrome P-450 reductase-paraquat, 7.4	1.2	N/A	N/A	N/A	N/A

[a]5-tert-Butoxylcarbonyl-5 methyl-pyrroline *N*-oxide, also known as BMPO.
[b]Not available.
[c]Apparent rate constant is relative to $k_{2,DMPO} = 60\ M^{-1}\,s^{-1}$.
Reprinted with permission from F.A. Villamena, et al. Reactivity of Superoxide Radical Anion with Cyclic Nitrones: Role of Intramolecular H-Bond and Electrostatic Effects. J Am Chem Soc 129, 2007, 8177.[24]

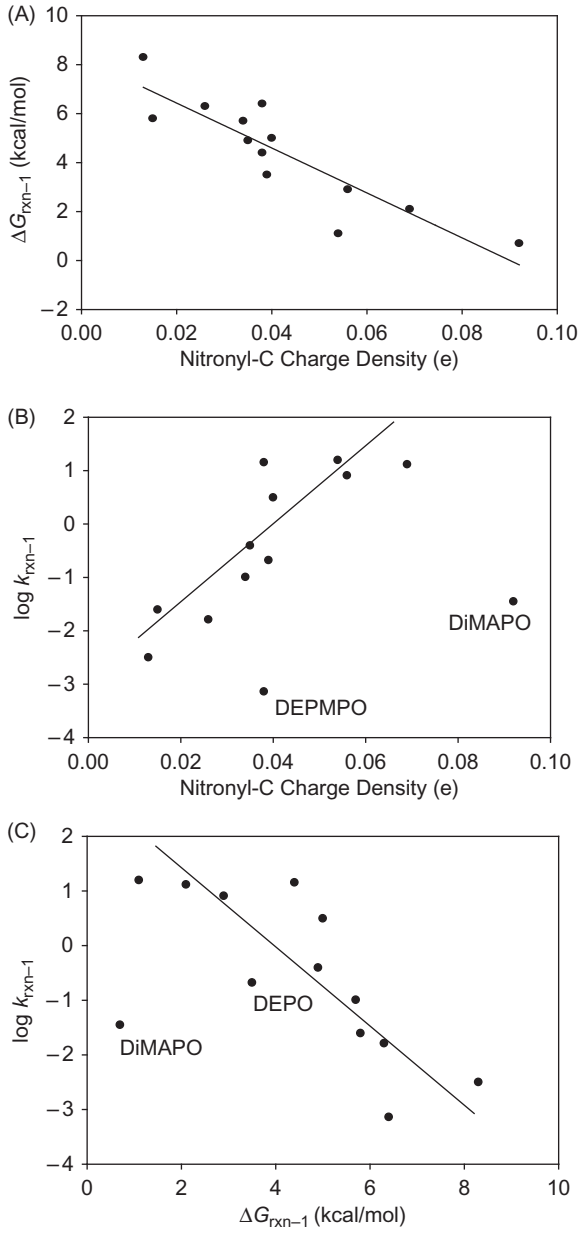

Figure 5.5 Correlation of the nitronyl-C (C-2) charge densities with that of the (A) free energies ($\Delta G_{rxn-1,298K}$, kcal/mol) ($r^2 = 0.78$); (B) rate constants (log k_{rxn-1}) of $O_2^{\bullet-}$ addition to nitrones in the aqueous phase at the PCM(water)/mPW1K/6-31 + G(d,p) level of theory at 298K ($r^2 = 0.76$, excluding the outliers DEPMPO and DIMAPO); and (C) shows the degree of correlation between log k_{rxn-1} and ΔG_{rxn-1} at the same level of theory with $r^2 = 0.73$, excluding the outliers DIMAPO and DEPO). *Reprinted with permission from F.A. Villamena, et al. Reactivity of Superoxide Radical Anion with Cyclic Nitrones: Role of Intramolecular H-Bond and Electrostatic Effects. J Am Chem Soc* ***129****, 2007, 8177.*[24] *Copyright © 2007 American Chemical Society.*

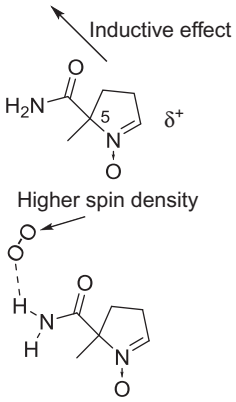

Figure 5.6 Two major effects of amide substituents on $O_2^{\bullet-}$ reactivity to nitrones.

due to the inductive effect by C-5 substitution with primary and secondary amide groups and (2) polarization of the electron distribution on $O_2^{\bullet-}$ by the amide N−H group via α-effect, which causes an increase in electron density of the terminal O and therefore increases $O_2^{\bullet-}$ reactivity to nitrones. This leads to an improved rate constant of 25 $M^{-1}s^{-1}$ compared to the absence of an amide group—i.e., 2 $M^{-1}s^{-1}$ for DMPO using the same spin-trapping conditions.[24]

More innovative spin traps that exploit these two important factors for increased $O_2^{\bullet-}$ reactivity had been synthesized. As shown in Fig. 5.7 e.g., having several hydroxyl groups cyclodextrin can increase H-bonding interaction with $O_2^{\bullet-}$ and was tethered to DMPO via an amide bond for increase positivity on the nitronyl-C, which led to increased rate of $O_2^{\bullet-}$ trapping to 60 $M^{-1}s^{-1}$ in comparison to DMPO of 2 $M^{-1}s^{-1}$.[47]

Since $O_2^{\bullet-}$ carries a negative charge, the use of an anion receptor that carries H-bond donors such as the pyrrole−NH calix[4]pyrrole may exhibit selectivity toward $O_2^{\bullet-}$. It was hypothesized that calix[4]pyrrole conjugation with spin traps can offer improved spin-trapping properties in terms of increased reactivity to $O_2^{\bullet-}$ and longer $O_2^{\bullet-}$ adduct half-life. Computational studies at the PCM/B3LYP/6-31 + G(d,p)//B3LYP/6-31G(d) suggest that a pendant-type linkage between the calix[4]pyrrole and the nitrone would be the most efficient design for spin trapping of $O_2^{\bullet-}$, giving exoergic reaction enthalpies ($\Delta H_{298K,aq}$) and free energies ($\Delta G_{298K,aq}$) of −16.9 and −2.1 kcal/mol, respectively, which are the first exoergic reaction energies ever observed for any nitrones studied thus far.[48] Using UV vis competitive stopped-flow kinetics in DMF/H_2O using KO_2 as $O_2^{\bullet-}$ source, the rate constant for the formation of the CalixMPO−$O_2^{\bullet-}$ adduct was approximated to be $k_2 = 680\ M^{-1}s^{-1}$ compared to AMPO of 130 $M^{-1}s^{-1}$, EMPO 105 $M^{-1}s^{-1}$, DMPO of 2 $M^{-1}s^{-1}$, and DEPMPO of 1 $M^{-1}s^{-1}$ (Fig. 5.8). Although the solubility of CalixMPO is limited in water, this is the highest rate constant observed so far for a

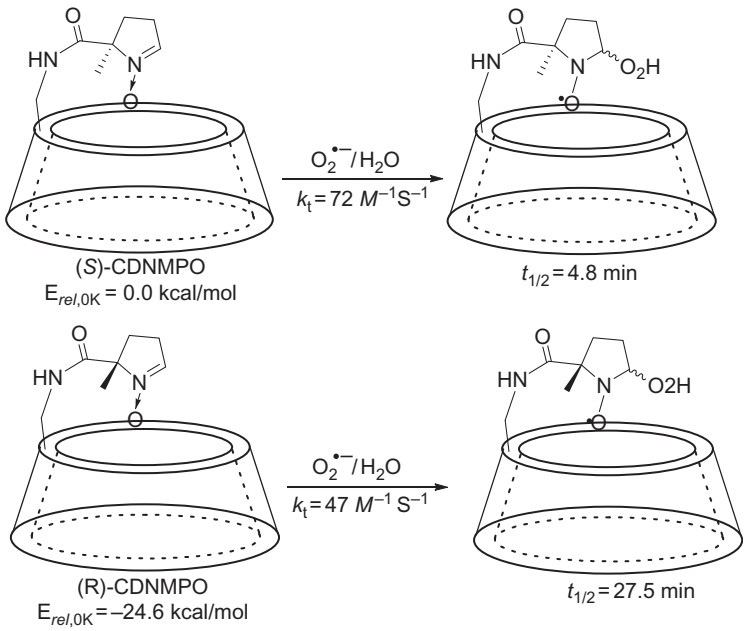

Figure 5.7 Spin-adduct formation from the two stereoisomeric forms of CD-MPO showing their rate constants of formation and half-lives. *Reprinted with permission from Han, Y. et al. Improved Spin Trapping Properties by beta-Cyclodextrin-Cyclic Nitrone Conjugate. J Org Chem* ***73****, 2008,7108. Copyright © 2008 American Chemical Society.*

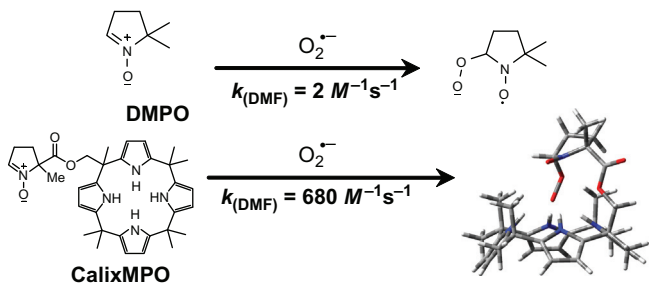

Figure 5.8 Comparison of the rate constants of formation of the superoxide adduct of DMPO versus CalixMPO. *Reprinted with permission from Kim S-U, Liu Y, Nash KM, Zweier JL, Rockenbauer A, Villamena FA. Fast Reactivity of Cyclic Nitrone-Calix[4]pyrrole Conjugate with Superoxide Radical Anion: Theoretical and Experimental Studies. J Am Chem Soc 2010;132:17157. Copyright © 2001 American Chemical Society.*

nitrone at the experimental conditions used in the study. The unusually high reactivity of CalixMPO to $O_2^{\bullet-}$ was rationalized to be due to the synergy between α- and electrostatic effects by the calix[4]pyrrole moiety on the $O_2^{\bullet-}$ and nitrone, respectively.

5.6 KINETICS AND THERMODYNAMICS OF ADDUCT DECAY

The half-life of nitrone radical adducts varies, depending on several factors, including (1) the nature of the radical trapped, (2) the nature of the spin trap, (3) solution pH,

(4) geometric isomerism, and (5) the presence of oxidoreductants. At neutral pH, the DMPO adducts of various radicals gave adduct half-lives ($t_{1/2}$) of 55 min[29] for $HO^{\bullet}$ and >1 h for C-centered ones, making these two spin adducts the easiest to detect in solution. However, the first-order decay half-life of DMPO adduct with $HO_2^{\bullet}$ is only 50 s.[25]

As a function of the spin trap, adducts such as DMPO−OH, EMPO−OH, BMPO−OH, DEPMPO−OH, and 5-diisopropoxyphosphoryl-5-methyl-1-pyrroline *N*-oxide−OH (DIPPMPO−OH) gave $t_{1/2}$ (min) = 55, 127, 37, 132, 158, respectively.[29] These reported experimental half-lives of $HO^{\bullet}$ adducts with various nitrones are relatively longer compared to their respective $HO_2^{\bullet}$ adducts—i.e., for DMPO, EMPO, BMPO, DEPMPO, and DIPPMPO, the $t_{1/2}$ (min) are ~1, 10, 9, 15, and 21, respectively.[21,38,49] The $HO_2^{\bullet}$ half-lives are therefore shorter compared to their $HO^{\bullet}$ adduct counterparts. Even when the $HO_2^{\bullet}$ adducts of 5-substituted spin traps impart longer half-lives compared to DMPO, these $HO_2^{\bullet}$ adducts are inherently less persistent and unstable in aqueous solution.[50] The $HO_2^{\bullet}$ adduct is known to decompose to the more persistent $HO^{\bullet}$ adducts. Several factors have been suggested to affect $HO_2^{\bullet}$ adduct stability such as presence of trace iron ions in solution, pH, and $O_2^{\bullet-}$ itself. A study by Buettner[50] suggests the dependence of $HO_2^{\bullet}$ adduct half-life on iron concentration where at concentrations of 1−100 μM of iron decomposition to the $HO^{\bullet}$ adduct occurs and at a faster rate at higher iron concentrations. The mechanism proposed for the generation of $HO^{\bullet}$ adduct was through the iron-catalyzed Haber-Weiss reaction where $HO^{\bullet}$ is generated from H_2O_2 and $O_2^{\bullet-}$, according to Eqs. (5.10)–(5.12):

$$Fe^{2+} + O_2^{\bullet-} \xrightarrow{H^+} Fe^{3+} + H_2O_2 \tag{5.10}$$

$$Fe^{2+} + H_2O_2 \rightarrow Fe^{3+} + HO^- + HO^{\bullet} \tag{5.11}$$

$$Fe^{3+} + O_2^{\bullet-} \rightarrow Fe^{2+} + O_2 \tag{5.12}$$

However, the presence of chelators such as ethylenediaminetetraacetate, diethylene triamine pentaacetic acid (DTPA), and deferoxamine did not prevent the decomposition of $HO_2^{\bullet}$ adducts or the formation of $HO^{\bullet}$ adducts.[50,51] Nevertheless, in spin-trapping experiments, buffers containing small amount of a chelator such as DTPA are recommended due to the metal-mediated nucleophilic addition reaction of water to nitrone, and its subsequent oxidation could produce the artifactual $HO^{\bullet}$ adduct, which will be discussed in detail in the succeeding section.

Solution pH has been shown to affect the $HO_2^{\bullet}$ adduct's half-life. According to Fig. 5.9, the half-life of DMPO-O_2H decreases in basic pH and is longest in acidic pH.[50]

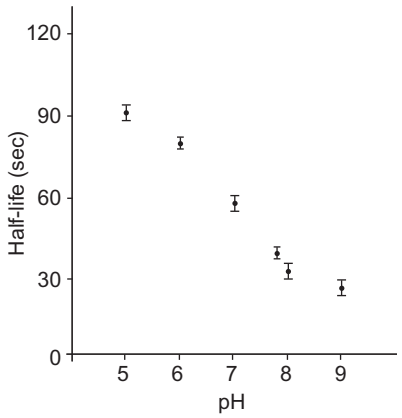

Figure 5.9 The half-life of the $HO_2^{\bullet}$ spin-adduct signal of DMPO in aqueous solution as a function of pH. (Adapted from G.R. Buettner and L.W. Oberley, *Biochem Biophys Res Commun* ***83****, 1978,69).*[50]

A threefold increase in the half-life of the $HO_2^{\bullet}$ adduct from pH 9 ($t_{1/2} = 27$ s) to pH 5 ($t_{1/2} = 91$ s) can be observed, and this trend is consistent with the pH dependence of $HO_2^{\bullet}$ adduct half-life of BMPO as well.[38]

Computational studies show that proton abstraction of the β-H of the $HO_2^{\bullet}$ adduct is highly exoergic with free energy of reaction of −78 kcal/mol (Eq. 5.13). However, EPR evidence for the formation of the keto-nitroxide is lacking, and the mechanism does not explain the short half-life regardless of the pH.[32]

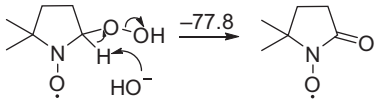

(5.13)

Thermodynamic instability of the adduct was then explained through its unimolecular decomposition via homolytic cleavage of the O−O peroxyl moiety and intramolecular ring opening to produce the nitrosoaldehyde and $HO^{\bullet}$. This reaction was found to be only slightly exoergic by 2.7 kcal/mol as shown in Eq. (5.14).[32] Using a different level of theory, the calculated unimolecular $\Delta G_{rxn,aq}$ of decomposition for DMPO−O_2H was found to be the most exoergic (−13.4 kcal/mol) compared to other $HO_2^{\bullet}$ adduct of various 5-substituted spin traps (−6.8 to 0.6 kcal/mol), but these values do not explain the trends in the relative stability between the adducts of these 5-substituted spin traps since DEPMPO−O_2H gave the most exoergic decomposition free energy of $\Delta G_{rxn,aq} = -4.7$ and −6.8 in this group when it is the most long-lived adduct among the spin traps studied.[52]

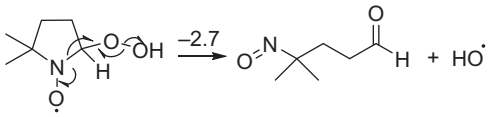

(5.14)

The redox properties of various nitrone−O_2H were then theoretically investigated,[53] and results show that *cis*- and *trans*-DEPMPO−O_2H gave the lowest electron affinity but the highest ionization potential, indicating that DEPMPO−O_2H is hardest to reduce and oxidize compared to the $HO_2^{\bullet}$ adducts of DMPO, EMPO, and AMPO, thus offering an explanation for the long half-life of DEMPO−O_2H in solution. In general, the IPs of $HO_2^{\bullet}$ adducts are higher compared to the more stable nitroxides such as 2,2,6,6-tetramethylpiperidine-*N*-oxyl (TEMPO), PROXYL, DMPO−OH, and DMPO−CH_3 adducts, which indicates a more facile oxidation for these latter class of nitroxides. The order of preference for nitroxide decomposition is via reduction by $O_2^{\bullet-}$ followed by oxidation by O_2 and then oxidation by $O_2^{\bullet-}$. Fig. 5.10 shows the thermodynamically preferred decomposition pathway for the one-electron reduction of nitrone−O_2H by $O_2^{\bullet-}$ via formation of the hydroxylamine and subsequent ring opening to form the aldehyde and concomitant elimination of HNO_2. For the one-electron oxidation of nitrone−O_2H by $O_2^{\bullet-}$, the preferred decomposition is the formation of the hydroxamic acid. This theoretical study predicts the redox properties of the nitrones and of the $O_2^{\bullet-}$ adducts as well as their subsequent decomposition to form biological active species such as NO, H_2O_2, and hydroxamic acid (Fig. 5.10).

Most of the adduct half-lives were obtained using chemical and enzymatic radical generating systems. While the half-lives of nitrone−O_2H could be enhanced by 5-substitution with electron-withdrawing groups, their half-lives in the presence of biological milieu are often times too short to be observable due to the susceptibility of the aminoxyl (nitroxyl) group of the spin adduct to be degraded by oxidoreductants and even by the radicals themselves. Application of spin trapping in the detection of $O_2^{\bullet-}$has been more successful at the enzymatic level using purified enzymes than using non-leukocyte cells. Stability of various spin adducts using different cyclic nitrones in the presence of Chinese hamster ovary (CHO) and 9L tumor cells was evaluated and, in the absence of cells, showed $t_{1/2}$ ranges of 19−90 min, 3−22 min, and 3−8 min for $SO_3^{\bullet-}$, $HO^{\bullet}$, and $^{\bullet}CH_3$ adducts, respectively. These half-lives were greatly reduced in cell suspension with $t_{1/2}$ ranges of 6−30 min, 1.5−5 min, and 1.5−5 min for $SO_3^{\bullet-}$, $HO^{\bullet}$, and $^{\bullet}CH_3$ adducts, respectively.[54]

The presence of methylated-cyclodextrin could increase the half-life of DMPO−O_2H and DEPMPO−O_2H in solution as previously demonstrated with the

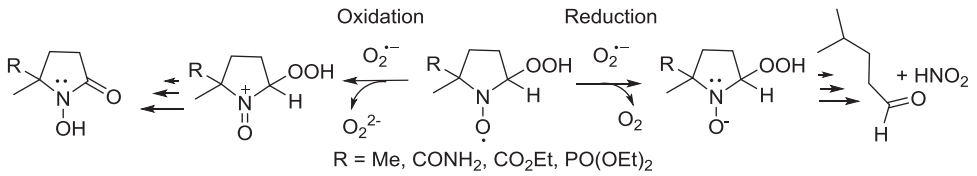

Figure 5.10 Mechanisms of nitrone−$O_2^{\bullet-}$ adduct decomposition after reduction and oxidation.

sevenfold increases in their half-lives.[55] The stabilizing effect of cyclodextrin was extended to esterified-nitrones with enhanced half-life in the presence of ascorbate.[56] And in some in vitro and most in vivo systems, $O_2^{\bullet -}$ production could only be deduced through the formation of HO-adduct and through additional control experiments involving SOD and catalase addition to show the origin of HO-adduct—i.e., whether from $O_2^{\bullet -}$ or H_2O_2, respectively.[57,58] Several methods, however, have been employed to increase nitrone$-O_2H$ half-life in solutions containing biological milieu—e.g., using EMPO and methylated-cylcodextrin or 2-hydroxypropyl-β-cyclodextrin, robust EMPO$-O_2H$ adduct formation was observed compared to without the aid of cyclodextrin.[59] Radical detection from endothelial cells is often times very difficult due to the low levels of radical produced on cell stimulation. Using the same EMPO−cyclodextrin system, the formation of C-centered $HO_2^{\bullet}$ and $HO^{\bullet}$ was observed from oxidatively challenged bovine aortic endothelial cells.[60]

Conjugation of DEPMPO with permethylated-β-cyclodextrin proved to increase the half-life of the HO_2-adduct by 250% (i.e., from 17 min for DEPMPO$-O_2H$ to 40 min for CD−DEPMPO$-O_2H$) in the absence of biological milieu.[61] Also, conjugation of nonmethylated-β-cyclodextrin with DMPO (CDNMPO) via amide bond showed enhanced HO_2-adduct half-life of approximately 30-fold from 1 min for DMPO$-O_2H$ to 27 min for CDNMPO$-O_2H$ in aqueous solutions.[47] Whereas, conjugation of DMPO with calix[4]pyrole (CalixMPO) gave an improved HO_2-adduct half-life in dimethyl sulfoxide (DMSO) of ∼25 min compared to DMPO$-O_2H$ of 6 min.[48] In the presence of rat liver microsomes, the of HO_2-adduct of nitrones−cyclodextrin conjugates—in particular, that of CD−DEPMPO and CD−DIPPMPO—showed half-lives of ∼80 and 110 min, respectively, similar in stability to that in the absence of microsomes. For the unconjugated-cyclodextrin spin traps, half-lives were significantly shortened in the presence of microsomes. All nitrones, however, showed diminished HO_2-adduct stability in the presence of rat liver cytosol.[62]

5.7 BIOSTABILITY AND CYTOTOXICITY OF SPIN TRAPS

Computational studies show that in general, electron-withdrawing group substituted nitrones at the C-5 position results in higher calculated electron affinity and ionization potential making them more susceptible to reduction but are more difficult to oxidize.[53] Fig. 5.11 shows the resonance structures of oxidized and reduced nitrones.

Cyclic voltammetric studies in aqueous medium reveal cathodic peak potential (V vs SCE) of −1.92 V for DMPO compared to −1.88 V for PBN,[63] indicating a more facile reduction for the latter. DMPO also exhibits high oxidation potential (vs SCE) of 1.63 and 1.47 V for PBN,[63] giving DMPO a wide potential window for application in biological systems. Therefore, in a biological system and given the range

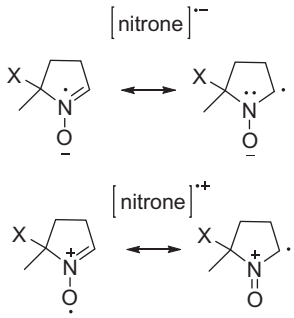

Figure 5.11 Resonance structures for the radical anion (top) and cation (bottom) showing the location of the unpaired electron.

of reduction potential for various oxidoreductants of 2.3 to −1.5 V (vs SCE),[30] it is expected that DMPO would generally be stable and that only those oxidants such as $HO^{\bullet}$ (2.31 V) or $CO_3^{\bullet-}$ (2.1 V)[64] with high reduction potentials above −1.92 V would be capable of oxidizing DMPO.

Nitrones have been shown to be tolerated in aortic endothelial cells with DMPO exhibiting the lowest toxicity with an IC_{10} of 86.8 mM compared to PBN of 5.4 mM after 24 h of incubation with highest toxicity for the nitroso compounds.[65] In a separate study using CHO cells, after 6 h of incubation no significant decrease in cell viability was observed using DMPO, BMPO, CMPO, EMPO, and DEPMPO in up to 50 mM concentrations except for BMPO, which gave significant toxicity at 50 mM and was only nontoxic up to 25 mM.[54] The effect of the spin traps on the number of colony formations of CHO and 9L-tumor cells was found to depend on cell type.[54]

The cytotoxicity of various derivatives of EMPO on different carcinoma cell lines also show BMPO to be the most toxic ($IC_{50} \sim 5-6$ mM) for all cell lines,[66] with DEPMPO and *i*-5-n-propyl-5-methyl-1-pyrroline-*N*-oxide (PrMPO) as the least toxic ($IC_{50} \sim 100-300$ mM) but dependent on cell line. The cell-type dependence of spin-trap toxicity, e.g., with DMPO was found to be only toxic to bovine pulmonary artery endothelial cells up to 1 mM but not toxic to lung microvascular endothelial cells up to 100 mM (unpublished data). Conjugation of an amphiphilic carrier to PBN and DMPO to form fluorinated amphiphilic PBN conjugate (FAPBN) and e fluorinated amphiphilic DMPO conjugate (FAMPO), respectively, only affects FAMPO toxicity but not FAPBN. FAMPO showed 20% and 50% decrease in cell viability at 0.5 and 1 mM after 24 h of incubation, respectively, while the carrier alone gave cell toxicity of 5−25%.[67] These results indicate that cellular permeability plays an important role on nitrone toxicity. Therefore, during spin trapping where cells are freshly harvested and the EPR spectrum is acquired immediately, toxicity would not be an issue.

In rats, DMPO was found to be not toxic up to 120 mg/100 g (w/w) compared to PBN with a lethal dose of 100 mg/100 g.[68] Evidence from gross pathology and

histopathological examinations showed that spin traps injected intraperitoneally gave no cellular damage—neither DMPO (232 mg/100 g by wt.) nor PBN (100 mg/100 g by wt)—while 4-PyOBN was found to be lethal at 100 and 200 mg/100 g by weight.[69] Spin trapping in vivo using DMPO was employed and found to have relative stability of 90 min after intraperitoneal injection (15 mmol/kg) in rats with concentrations high enough to trap C-centered radicals. After 2 h, 40% of the injected DMPO was still available. However, only the more stable adduct—i.e., the C-centered ones—could be detected since the half-life of DMPO-OH was too short to be observed, disappearing after 1 min of its generation.[70] In spite of the in vivo application of spin trapping using DMPO, $O_2^{\bullet -}$ production has also been indirectly observed as an $HO^{\bullet}$ adduct (see Table 5.3).

5.8 SYNTHESIS OF SPIN TRAPS

The general synthesis of nitrones is shown in Scheme 5.2. Several review articles, books, and papers have appeared over the years describing the general synthesis of nitrones.[71–74] The most efficient routes to synthesize nitrone functionality are by condensing carbonyl compounds with hydroxylamine and oxidizing amine, imine, or hydroxylamine moieties.

Reaction I. The reaction proceeds via condensation of the aldehyde or ketone with hydroxylamine to give aldonitrone or ketonitrone, respectively, but often yields crude products that are difficult to separate.[75]

Reaction II. For cyclic or DMPO-type nitrones, this procedure will typically involve the synthesis of aldo–nitro or keto–nitro compounds via a Michael addition reaction of a nitroalkane (i.e., 2-nitropropane) to activated olefins such as α,β-unsaturated carbonyl compounds. Subsequent reductive cyclization using

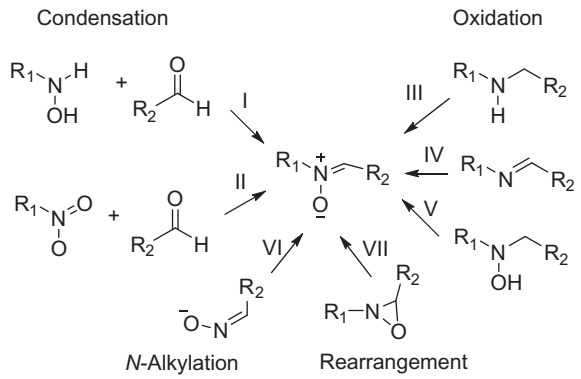

Scheme 5.2 Various routes for nitrone synthesis.

reducing agents such as Zn metal in acidic conditions forms the nitrone.[76] In some cases, it is necessary to protect the aldehyde as an ethylene−glycol acetal[38,43,77,78] to minimize side reactions. Selective reductive coupling of nitro compounds with aldehydes to nitrones could also be accomplished in H_2 using carbon-supported Pt nanoparticles.[79]

Reaction III. Oxidation of secondary amines is usually carried out with H_2O_2 using molecular sieves;[80] Na_2WO_4[81] and SeO_2,[82] as catalysts; alkyl hydroperoxides and titanium alkoxides as catalyst;[83] or with mCPBA.[84]

Reaction IV. Imines can be oxidized to nitrones by dioxiranes such as dimethyldioxirane[85] and methyl(trifluoromethyl)dioxirane[86,87] or oxidation by peroxyacid.[85] Imines can be reduced to amine with $NaBH_4$ followed by oxidation with H_2O_2/Na_2WO_4 to nitrones.[88]

Reaction V. Oxidation of hydroxylamines to nitrones can be carried out using bleach,[89] MnO_2,[90] H_2O_2 catalyzed by methylrhenium trioxide $MeReO_3$ [91], or $Cu(OAc)_2/O_2$.[92]

Reaction VI. Benzaldoxime is *N*-alkylated by various alkyl halides to form the nitrone, however, consideration of geometric isomerism and steric factors is important due to the formation of O-alkylated products.[93]

Reaction VII. Oxaziridines prepared from the oxidation of imines by *m*-chloroperoxybenzoic acid can undergo thermal rearrangement to form the corresponding nitrones and can be catalyzed by Lewis acids.[94]

5.9 INTERPRETATION OF EPR SPECTRA

Spin-trapping EPR spectra could provide a myriad of information about the identity, molecular size, and nature of the radical species being trapped as well as their concentration. Three important pieces of information can be obtained from the *x*-axis.

First, the *g* value provides information into the nature of the radical species (e.g., organic versus metal-based). For the spin adducts, the solution *g* value is typical of aminoxyl compounds ($g = 2.006$)[95] with *g* values ranging from 2.005 to 2.007.[28,96−98]

Second, hyperfine splitting (or coupling) constant is the most informative spectral parameter in EPR spin trapping such that it provides information about the identity of the radical being trapped. The interaction of the unpaired electron with the nuclei of the trapped radical that is bound to the C-2 gives rise to additional splitting patterns for the magnetic nuclei or shows that it could also result in variations in the hyperfine splitting constants of the nitronyl-N and β-hydrogen as shown in Table 5.2. Noteworthy is the $a_N/a_H = 1$ observed for the $HO^{\bullet}$ adducts generated from various radical generating system and $a_N/a_H = 1.21-1.27$, which is unique for $HO_2^{\bullet}$, depending on the $O_2^{\bullet-}$-generating system used. The smallest a_N/a_H ratio of 0.65−0.71 can be observed for the C-centered adducts for phenyl, phenyl-substituted, and alkyl radicals.

Table 5.2 Survey of the various hyperfine splitting constants observed for various spin adducts of DMPO in aqueous solution[a]

Trapped radical	a_N (G)	$a_{\beta\text{-H}}$ (G)	Additional a_x (G)	a_N/a_H	Ref
$^{\bullet}H$	16.0–16.6	21.5–23.2 (2 H's)		0.70–0.75	
$^{\bullet}C_6H_5$-X	15.0–15.4	21.2–25.0		0.65–0.70	
$^{\bullet}R$	14.9–16.5	19.6–24.1		0.68–0.71	
$^{\bullet}CONH_2$	15.5	20.5		0.75	
$^{\bullet}CO_2^-$	15.7	18.7		0.84	99
$^{\bullet}OCO_2^-$	14.3	10.7	1.37 (γ-H)	1.33	100
$^{\bullet}OH$	14.3–15.0	14.3–15.0		1.0	
$^{\bullet}NH_2$, $^{\bullet}NHR$	15.6–15.9	18–19.3	1.6–2.5 (N)	0.82–0.86	
$^{\bullet}NHCOR$	15.4	20.3	2.4 (N)	0.76	
$^{\bullet}N_3$	14.5–16.9	14.5–16.9	3.0–3.2 (N)	1.00–1.05	101
$^{\bullet}O_2R$	14.25–14.5	10.5–11.5	1.1–1.25 (γ-H)	1.28–1.38	
$^{\bullet}O_2H$	13.8–14.4	11.1–11.7	1.22–1.37(γ-H)	1.21–1.27	
$^{\bullet}OR$	14.5–15.0	15.7–16.7		0.89–0.93	
$^{\bullet}SH$, SR	15.1–15.4	16.2–18.0		0.89–0.94	
$^{\bullet}SO_3^-$	14.5–14.7	15.9–16.5		0.89–0.91	102
$^{\bullet}OSO_3^-$	13.7–13.9	10.1–10.5	1.3–1.5 (γ-H)	1.36–1.37	102
DMPO-X	7.0–7.2	4.0–4.2		1.69–1.71	

[a]All the values were taken from the Spin Trap Database by the National Institute of Environmental Health Sciences and their respective references can be obtained therein. Additional references are provided.

Moreover, hyperfine splitting constants are strongly influenced by the solvent polarity where protic solvents results in higher hyperfine splitting constants (HFSCs) compared to aprotic solvents.[103]

Third, the line width and shape of the spectrum are affected by the molecular size of the trapped radical, intermolecular attractive forces such as H-bonding between adducts, or viscosity of the solution, giving information on the local molecular tumbling or rotational dynamics. Moreover, the presence of conformational isomerism and, in the case of 5-substituted nitrones, geometric isomerism also contributes to line width and shape of the spectrum.

In general, EPR spectra resulting from spin trapping are all isotropic because of the fast tumbling motion of the molecules, which allows for the averaging of the rotational motion and hence gives more symmetrical line patterns. However, small differences in the spectral profile can be observed such as the ones shown in Fig. 5.12 in which the type of trapped radical has a drastic effect on the hyperfine splitting pattern as well as line width of the spectrum of the adduct formed. Although the molecular size of each trapped radical is approximately the same, their conformational and inductive effects as well as their ability to exhibit intermolecular interaction could

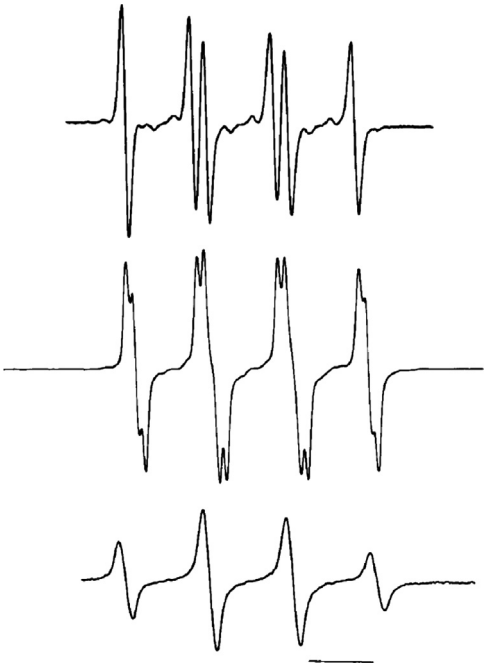

Figure 5.12 EPR spectra of DMPO thiyl adducts from (top) 2-methyl-2-propanethiol, (middle) α-toluenethiol, and (bottom) 2-hydroxyethanethiol.[104] *(*Adapted from Josephy et al. *Tet Lett 1984;**25**:1685).*

affect spectral profile. The line width broadening for 2-hydroxyethanethiol-adduct could be the result of a strong H-bond interaction between the adducts, and that can hinder molecular tumbling motion (which is more evident at the highest field peak), so the hyperfine splitting pattern resulting from the β-H as seen from 2-methyl-2-propanethiol- and α-toluenethio-adducts was obscured.

The effect of molecular size on the EPR spectrum of thiyl adducts is shown in Fig. 5.13. Comparison of DMPO−glutathione disulfide (DMPO-SG) and DMPO-SHb (hemoglobin thiyl adduct) shows a much broader line width for the latter, although still in the fast motion regime, which indicates a slower rotational motion (τ_c) compared to the former.

Because a spectral profile is influenced by several of the factors just mentioned, it is possible to rationalize the origins of hyperfine splitting patterns using a computational approach[106] or by isotopic labeling.[107] Fig. 5.14 shows the characteristic spectral profiles exhibited by various DMPO spin adducts. Of particular interest is the distinctive spectrum exhibited by DMPO−OH compared to that of DMPO−O_2H in spite of the very small difference in their chemical compositions—i.e., the latter has only one more oxygen atom than the former. Aside from the difference in the $a_N/a_{\beta\text{-H}}$ ratio of DMPO−OH and that of DMPO−O_2H, the presence of additional splitting

Figure 5.13 EPR spectra of DMPO-SG adduct generated after 1 minute of Hg/Xe light irradiation of (A) 10 mM DMPO and 50 mM GSSG and (B) DMPO-SHb generated 30 min after addition of 175 μM phenylhydroxylamine in 20% intact rat red cell suspension containing 100 mM DMPO.[105] (Adapted from Bradshaw et al. *Free Radic Biol Med 1995;**18**:279).*

due to γ-H (i.e., hydrogen attached at the 3- or 4-carbon position) of ~1.2−1.4 G (see Table 5.2) gives rise to a 12-line spectrum that is distinctive of the DMPO−O_2H. However, extensive spectral simulation and low-level quantum mechanical calculations led to the proposition that the additional splitting pattern in the spectrum of DMPO−O_2H was due to the overlapping spectra from two different conformers of DMPO−O_2H and not from γ-H splitting.[108] Deuterium isotopic labeling of the γ-H's at C-3 only gave a six-line spectrum, confirming ~1.2 G contribution of γ-H's to the hyperfine structure.[107] Density functional theory approach showed that only the $a_{\beta\text{-H}}$ is sensitive to conformational changes of the −OOH moiety and that both γ-H's that are *syn* and *anti* to −OOH gave the highest HFSC (1.1−1.3 G) compared to other γ-H's attached at C-4,[106] further confirming the contribution of these H's to the hyperfine structure. In addition to the conformational effects to the hyperfine structure, the presence of diastereoisomers[29,109] in the case of 5-substituted DMPO analogs such as DEPMPO can give rise to line asymmetry and line-width broadening as shown in Fig. 5.14 for the various spin adducts of DEPMPO, further complicating spectral interpretation.[110]

Qualitative spectral analysis focuses mainly on the identification of the radical trapped. Hyperfine splitting patterns as well as the line shape and width of the spin-adduct spectrum serves as a spectral fingerprint that can provide information into the

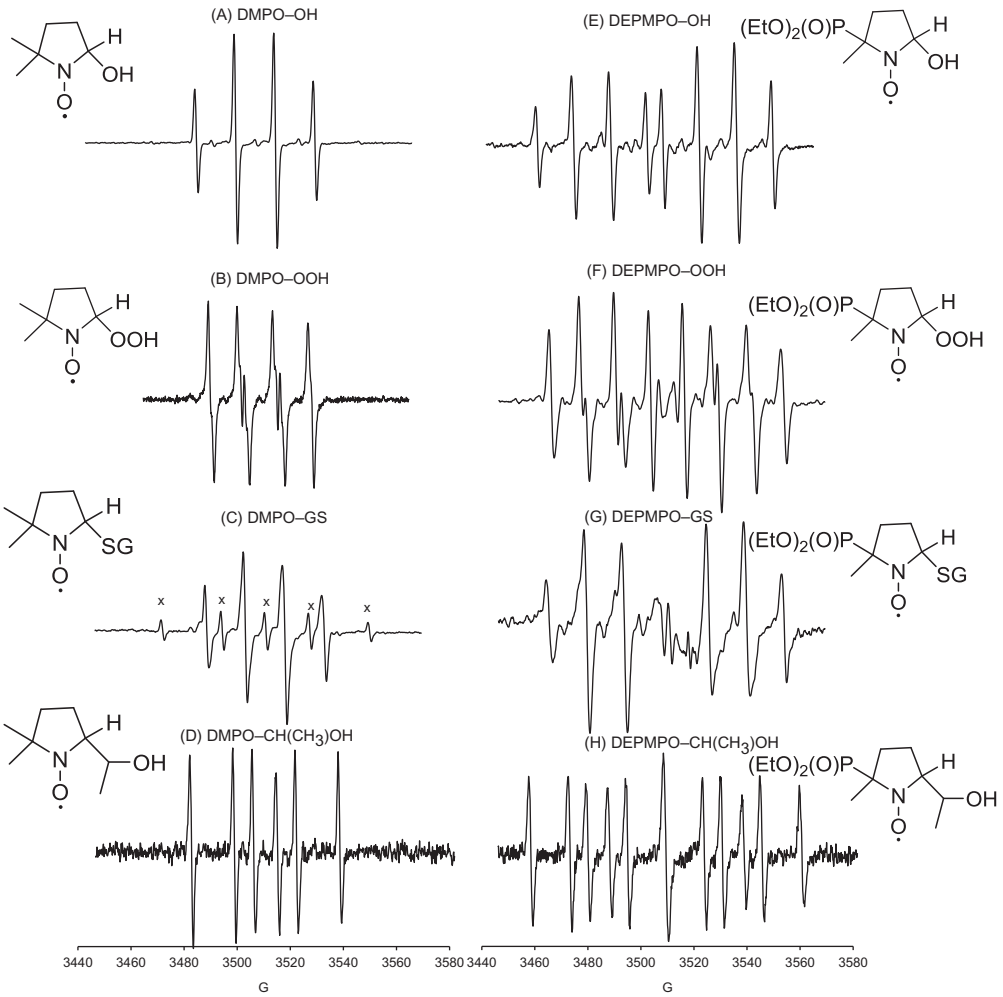

Figure 5.14 EPR spectra of various adducts of DMPO and DEPMPO *(*Adapted from Villamena, F. A. *Antioxid Redox Signal* ***6****, 2004, 619)* .[111]

nature, type, and identity of the radical. Typically, the isotropic solution spectrum is simulated using the following software:

1. WinSim—This public domain software is available from the National Institute of Environmental Health Sciences, Public Electron Paramagnetic Resonance Software Tools. It is intended for EPR simulations of experimental isotropic spectra—either the continuous wave (CW) or the fourier transform (FT) spectrum. The program can simulate as many as 10 species at varying concentrations, with each species containing 16 magnetic nuclei.[112]
2. EasySpin—This MATLAB-based application developed by Dr. Stephan Stoll.[113]

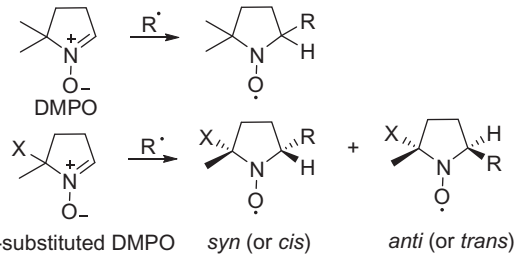

Figure 5.15 Comparison of formation of various adducts from DMPO and 5-subtituted nitrone

3. ROKI—This DOS-based application was developed by Professor Antal Rockenbauer.[114]

The type of spin traps and the relative concentration of spin adducts are considered during simulation. The use of DMPO simplifies spectral analysis such that it avoids consideration of diasterioisomer formation, so there are fewer species to consider in the simulation. Typically with DMPO, only one species is considered, but with 5-substituted nitrones such as EMPO, DEPMPO, BMPO, and AMPO, because radical addition is not regiospecific, the presence of diastereoisomers are inevitable as shown in Fig. 5.15.

The relative concentrations of the spin adducts generated from two or more type of radicals as well as formation of diastereomeric adducts can vary and could primarily affect the line shape and width of the spectrum. Slight differences in the *g*-factor of the various adducts formed can also affect overall spectral profile. Simulation of spectral parameters should give optimized parameters for each species such as hyperfine splitting constants for relevant atoms, *g*-factor, line width, and fractional amount of the species.

Quantitative analysis of spin adducts can provide important information about the kinetics and favorability of radical production. The rate of radical production can be measured by competitive kinetic techniques using enzymatic or chemical systems as mentioned elsewhere.[25,37,38,41] While these techniques mostly assess the rate of $O_2^{\bullet -}$ trapping of newly developed spin traps, in principle they can be employed to study kinetics of radical production from cells, but none of those have been carried out yet. In determining the rate of radical reaction by an antioxidant (new spin traps or non−spin traps alike), competitive kinetic technique uses a known radical scavenger (e.g., for $O_2^{\bullet -}$, SOD, ferricytochrome c, or DMPO) whose rate constants for $O_2^{\bullet -}$ trapping are known and the relative rates are then calculated. Radical production can be initiated, depending on the nature of radical generation. Photolysis and stopped-flow technique allow for the acquisition of critical initial rates of radical formation since the sample is already positioned in the cavity before radical production commences. In cases when it is impractical to initiate radical production in the EPR cavity, radical initiator is added first into the tube and the sample holder is immediately placed inside the cavity. However, by doing so, critical time is lost during sample

placement in the cavity and microwave tuning, therefore, this technique is not recommended for fast reactions such as studying the rate of $HO^{\bullet}$ production, although this technique is reasonable for studying the rate of $O_2^{\bullet -}$ reaction due to the slower production of $O_2^{\bullet -}$ and its reaction to spin traps.

Data acquisition can be carried out in two ways: (1) by using time scan at constant field where the growth of either the first or second low-field peak is monitored over a period of time provided a stable magnetic field and (2) by an incremental field sweep in which the whole or part of the spectrum is repetitively recorded over time. With time-scan acquisition, the initial rate of reaction is determined from the slope of peak amplitude (or intensity) as plotted against time, while with incremental field sweep, peak intensity, or area of a selected peak or of the whole spectrum is determined and plotted against time. Quantitation of radical production employs a standard curve of stable nitroxide such as TEMPO or proxyl nitroxides whose double integrated area of a peak or whole spectrum or peak amplitude of the low-field peak is plotted against a range of concentrations ($\sim 0.1-10\ \mu M$ in buffer).[115]

5.10 APPLICATIONS OF SPIN TRAPPING

There are three major scenarios in radical detection using EPR spin trapping: (1) no signal, (2) weak signal, and (3) strong signal. The major limitation in radical detection using spin trapping is the quantity of radicals being produced by the system. The presence of biological milieu, which drastically shortens the adduct half-life, is perhaps the most significant setback in the application of spin traps for biological radical detection. Furthermore, the detection of $O_2^{\bullet -}$ is even more difficult due to its slow reactivity to spin traps and its inherently short half-life. Therefore, the absence of EPR signal during spin trapping may not necessarily indicate that radicals were not generated but could be due to any of the factors previously mentioned. Conversely, the presence of a signal does not necessarily indicate radical production. However, several experimental "tricks" and procedures have been developed to overcome these shortcomings.

1. *Avoid basic pH conditions.* Spin-adduct half-life is shortest in basic conditions as mentioned previously and, therefore pH conditions between normal physiological pH and below would be appropriate for spin trapping.
2. *Sequester trace amounts of transition metal ions.* Artifacts are commonly encountered in spin-trapping experiments. The metal-catalyzed Forrester-Hepburn mechanism shown in Eq. (5.15) has been proposed as a nonradical pathway for adduct formation and could be misleading.[116] Formation of DMPO−OH adduct due to the nucleophilic addition of H_2O in the presence of Fe^{III} or Cu^{II} was confirmed using ^{17}O-enriched water. While catalase does not affect this adduct formation, the presence of metal chelators exerts inhibition. Because metal impurities are only present at submicromolar levels, nonradical metal-mediated reactions can be

significantly minimized through the use of chelating agents showing both DTPA and nitrilotriacetic acid to effectively prevent DMPO−OH formation in the presence of high-valent transition metal ions.[117] Typically, buffer solutions containing 100 μM of DTPA is a reasonable precautionary measure for carrying out spin trapping under biological conditions.

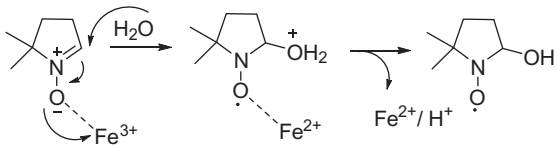

(5.15)

3. *Proper choice of media.* Sometimes mixed solvents are necessary to solubilize reagents such as drugs or newly developed spin traps used for radical generation. When the formation of O-centered radicals is desired, it is desirable to use solvents that do not form C-centered radicals. Secondary radical adduct formation from H-atom abstraction from solvents by $HO^{\bullet}$ can complicate spectral interpretation. Heats of reaction (ΔH) of H-atom abstraction from various solvents by $HO^{\bullet}$ in water at 300 K shows the following order of increasing exoergicity: CH_3CN (3.7) < CH_3CH_2OH (−2.8) < CH_3OH (−3.5) < $(CH_2OH)_2$ (−8.1) < $(CH_3)_2CHOH$ (−8.5).[118] In general, the use of acetonitrile (CH_3CN) could minimize C-centered adduct formation. Also recommended is the use of phenol red free cell culture media (preferably just plane buffer) because phenol red can also compete with spin traps for radicals, especially that of $O_2^{\bullet -}$.[20]
4. *Sequence of reagent addition matters.* Knowing the molecular basis of radical production would aid in the design of successful protocols for radical detection. Due to the very short half-lives of radicals, having the spin trap in solution before initiating radical production increases the chance of detecting spin adducts. Examples of radical initiators are visible light for a riboflavin system to form $O_2^{\bullet -}$; UV for the homolytic cleavage of disulfides and peroxides to formthiyl and alkoxyl radicals, respectively; electric current for electrochemical generation of radicals; chemicals such as KO_2 or 3-morpholino-sydnonimine (SIN-1) to generate $O_2^{\bullet -}$ or peroxynitrite, respectively; substrates such as xanthine for xanthine oxidase; cell activators such as lipopolysaccharide (LPS), menadione, phorbol 12-myristate 13-acetate (PMA), or calcium ionophore; enzyme could also be an initiator such as xanthine oxidase or horseradish peroxidase; and O_2 in hypoxia and reoxygenation models.

   The most obvious source of free radicals such as O_2 is often overlooked in spin trapping where its presence is necessary for radical production. Bubble air or pure oxygen in solution can increase radical production particularly in radical generating systems such as light/riboflavin, NADPH oxidases, xanthine/xanthine oxidase. Use of appropriate light source is necessary to generate free radicals such that one would not use visible light to generate $HO^{\bullet}$ from H_2O_2.

5. *Toxicity of spin traps*. As mentioned previously, although spin traps are mostly non-toxic, their toxicity depends on the spin trap and cell type. When working on new cell lines that have not been investigated for spin trapping, it is advisable to do quick colorimetric cell viability studies using tetrazolium dye, 3-(4,5-dimethylthiazol-2-yl)-2,5-diphenyltetrazolium bromide (MTT assay) , or lactate dehydrogenase cytotoxicity assays.
6. *Choice of spin trap.* For the detection of $O_2^{\bullet -}$, because the rates of trapping by commercially available spin traps are pretty much the same, the choice will greatly depend on the spin trap that will impart the longest $O_2^{\bullet -}$ adduct half-life. Typically, EMPO, BMPO, or DEPMPO are the nitrones of choice. For more reactive radicals such as OH, C-centered or thiyl radicals, the choice of spin trap is probably not that important for the most part because the rate constants are of the same orders of magnitude with all of the commonly used nitrones, and their relative spin-adduct half-lives are long enough to be detected by EPR. The choice between PBN and cyclic nitrones will depend on whether one wants to perform in vivo spin trapping of free radicals utilizing ex vivo detection since the use of PBN is more established and tested than DMPO for this type of application.[119]
7. *Type of cell lines*. All cell types have distinctive biological roles and, therefore their ability to generate radicals could vary from one type to another. Although spin trapping has been employed on various cells such as endothelial cells[60,120] and epithelial cells[121] and bacteria,[122] radical generation from leukocytes had been shown to be the most robust such for neutrophils[123] or monocytes and macrophages.[124,125]
8. *Integrity of samples and spin traps used*. Enzyme activity should be carried out to assess enzyme viability. Cells must be freshly cultured, detached, pelletized, and resuspended in an appropriate medium (preferably just buffer) before any spin-trapping experiment. A cytotoxicity assay to test spin-trap toxicity on cells must also be carried out. Pure spin traps or aliquot solutions should be stored at least at −20°C or at −80°C for long-term storage. Spin traps could be degraded with long-term exposure to light, heat, air, or metals ions. Although spin traps are sold and advertised as 99.9% pure, some of the commercially available spin traps sometimes have paramagnetic impurities and therefore the EPR spectrum of the solution of the spin trap alone should first be tested for the presence of paramagnetic impurities before starting actual studies. One should note that the typically sensitivity of EPR for nitroxides is $\sim$ 1-10 μM and therefore a 50 mM spin trap with a 1% paramagnetic impurity would give a signal that could greatly interfere with the rest of the spectrum. Spin traps could also contain hydroxylamine as impurity and could produce nitroxide on exposure to O_2 or other oxidizing agents in the solution. Aside from running an EPR spectrum of

the spin-trap solution alone, one should also run a positive control experiment of the nitrone using a well-established radical-generating system such as the Fenton system composed of 1−100 μM Fe^{2+} and 0.1−10 mM H_2O_2.

9. *Miscellaneous issues.* Before planning any experiment, instrument should be tested to ensure that it is working properly by running a spectrum of a known solution of stable nitroxides such as that of TEMPO. Critically couple the cavity by properly positioning the sample, locating the microwave frequency, adjusting the iris screw for better coupling, or increasing the microwave energy. Depending on the radical-generating system being used, optimize the EPR experimental parameters such as receiver gain, modulation amplitude, time constant, and scan rate. Choose the appropriate sample cell to be used. For example, standard 50-μL glass microhematocrit capillary tube is typically used for spin-trapping experiments in aqueous solutions where one end of the tube is sealed by synthetic wax sealant (white synthetic wax is preferred to the brownish clay sealant because the latter contains paramagnetic manganese ions that interfere with the spectrum), but they are not preferred for UV irradiation where quartz capillary tube is used instead and is commercially available. Quartz sample tube (135−250 mm long × 4 mm outside diameter, where the longer one is used with finger dewar) is preferred for solid samples and organic liquids with lower dielectric constants ($\varepsilon = 2-4$). Flat cell (10 mm) is used for solvents with high dielectric constants and is preferable for the study of radical production from cells because this allows for the use of higher volume (at least 300 μL) and cell density needed to achieve upper limits of radical production.
10. *Use of control experiments*. To exclude nonradical pathway for spin-adduct formation, adding SOD and catalase before initiating radical production should inhibit $O_2^{\bullet-}$ and $HO^{\bullet}$ (via H_2O_2) adduct formation, respectively. Ethanol, methanol, or DMSO can also be added to confirm the generation of $HO^{\bullet}$ via formation of alcohol-derived secondary C-centered radicals. Since DMPO-OOH has a short half-life and is known to decompose to DMPO−OH, performing competitive experiments with alcohols, DMSO, and catalase could verify the origin of DMPO−OH—i.e., from DMPO−OOH decomposition or direct addition of $HO^{\bullet}$ to DMPO. Also, due to the instability of the primary peroxyl radical, conversion to its corresponding alkoxyl radical adduct could occur. For example, in the case of polyunsaturated fatty acid (PUFA) peroxyl radicals could gave rise to PUFA-derived alkoxyl radical adducts rather than the expected primary PUFA peroxyl radical adducts, thus complicating spectral interpretation.[126]

Since $O_2^{\bullet-}$ is the major precursor of the more highly oxidizing (or reducing) reactive species, its detection is highly desirable but also the most challenging. Shown in Table 5.3 are the various systems in which $O_2^{\bullet-}$ has been directly (or indirectly) detected using spin trapping, which includes chemicals, enzymes, organelles, cells, organs (tissues), and whole animals. The ease of $O_2^{\bullet-}$ detection is more evident from

Table 5.3 Survey of the various chemical, enzymatic, organelle, cellular, and in vivo systems in which radical generation has been detected using EPR spin trapping

System	Method	Spin trap	Radical detected	Ref
Chemical				
Fullerenes	Ultraviolet A (UVA) irradiation with or without nicotinamide adenine dinucleotide (NADH) addition	DMPO	$O_2^{\bullet-}$	127
Phenanthraquinone	P450 reductase, NADPH	DMPO	$O_2^{\bullet-}$, $HO^{\bullet}$	128
Dichlorofluorescein	Oxidation by horseradish Peroxidase, NADH	DMPO	$O_2^{\bullet-}$	129
Cyanine dyes	Irradiation at 350-nm light	DMPO	$O_2^{\bullet-}$, $HO^{\bullet}$	130
Advanced glycation end products	UVA irradiation	DMPO	$O_2^{\bullet-}$	131
Aqueous cigarette extract	Incubation in air saturated DMSO or water	DMPO	$O_2^{\bullet-}$, $HO^{\bullet}$	132
Curcumin	420-nm irradiation in benzene	DMPO	$O_2^{\bullet-}$, $HO^{\bullet}$	133
Enzymatic				
eNOS	NADPH, Ca^{2+}, calmodulin	DMPO	$O_2^{\bullet-}$	134
nNOS	NADPH, Ca^{2+}, calmodulin	DMPO	$O_2^{\bullet-}$	135–137
iNOS	NADPH, Ca^{2+}, calmodulin	DMPO	$O_2^{\bullet-}$	58,138
Soybean lypoxygenase	Linoleic acid	DMPO	$HO^{\bullet}$, $O_2^{\bullet-}$, $RO^{\bullet}$, $R^{\bullet}$	139
Cell wall–bound peroxidase	Incubation	DEPMPO	$O_2^{\bullet-}$, $HO^{\bullet}$	140
Xanthine oxidase	Xanthine	DMPO	$O_2^{\bullet-}$, $HO^{\bullet}$	50
Aldehyde oxidase	NADH	DEPMPO	$O_2^{\bullet-}$	141
Fe^{3+}cyt c	NADH, H_2O_2	DMPO, Me-β-CD	$O_2^{\bullet-}$	142
Complex I (NQR)	NADH	DEPMPO	$O_2^{\bullet-}$	143
Succinate-cytochrome c reductase	Succinate	DEPMPO	$O_2^{\bullet-}$	144
NADH dehydrogenase	NADH	DEPMPO	$O_2^{\bullet-}$	145

Organelle				
Intact mitochondria	Succinate	DEPMPO, mito-DEPMPO	$O_2^{\bullet -}$	146
Microsomes	Uroporphyrin, NADPH	DMPO	$O_2^{\bullet -}$, $HO^{\bullet}$	147
Chloroplast	Light photolysis in the presence of O_2	DMPO	$O_2^{\bullet -}$	148
Thylakoid membranes and PS II core particles	White light illumination	EMPO, Me-β-CD or HP-β-CD	$O_2^{\bullet -}$	59
Cellular				
Neutrophils	PMA	DMPO	$O_2^{\bullet -}$	149
	Chemotactic peptide, formylmethionylleucylphenyl-alanine	DMPO	$O_2^{\bullet -}$	147
Macrophages (RAW 264.7 cells)	LPS, PMA	DMPO	$HO^{\bullet}$	58
Human mammary epithelial cells (MCF-10A cells)	1,6-Benzo[a]pyrenequinone	DMPO, BMPO, DEPMPO, DEPPEPO	$O_2^{\bullet -}$	121
Microglial cells	Opsonified zymosan	DEPMPO	$O_2^{\bullet -}$, $HO^{\bullet}$	150
Osteoclasts	NADPH	DMPO	$O_2^{\bullet -}$ as $HO^{\bullet}$	151
Endothelial cells	O_2 purge	DMPO	$O_2^{\bullet -}$, $HO^{\bullet}$	152
	Anoxia or reoxygenation	DMPO	$O_2^{\bullet -}$, $HO^{\bullet}$	57,153
	SIN-1 treatment, then Ca I	EMPO, Me-β-CD	$O_2^{\bullet -}$, $HO^{\bullet}$, $R^{\bullet}$	60
Organ (perfusates)				
Rat liver	I/R	DMPO	$O_2^{\bullet -}$, $HO^{\bullet}$	154
Rat heart	I/R	DMPO	$O_2^{\bullet -}$, $HO^{\bullet}$, $R^{\bullet}$	155,156

(*Continued*)

Table 5.3 (Continued)

System	Method	Spin trap	Radical detected	Ref
Animal (ex-vivo)				
Humans	Excised skins; UVA, UVB, or UVC irradiation	DMPO	$R^{\bullet}$, $RO^{\bullet}$	157
Rabbits	Injury-induced excised aorta, NADH, NADPH	DMPO	$O_2^{\bullet -}$ as $HO^{\bullet}$	158
Rats	Blood, excessive resistive loading of the respiratory muscles	PBN	$R^{\bullet}$	159
	Bile and urine samples, ethylene glycol poisoning	POBN	$^{\bullet}[^{13}C]$Et-Glycol radical	160
	Lung extracts of intratracheally instilled asbestos	POBN	$R^{\bullet}$	161
Swine	Blood, ischemia, and reperfusion of the heart	PBN	$RO^{\bullet}$	162
Mice	Brain, spleen, and liver lipid extracts after gamma irradiation	PBN	$R^{\bullet}$	163
	Skin, topical treatment with phenol	PBN	$R^{\bullet}$	164

chemical to leukocytic cellular systems. Superoxide detection in cells other than leukocytes can be aided through the use of adduct stabilizing agent such as the permethylated-β-cyclodextrin (Me-β-CD). However, with tissues, the robustness of $O_2^{\bullet -}$ adduct formation diminishes and is mostly detected as secondary C-centered and alkoxyl-adducts in ex vivo measurements from animals. From cellular systems to in vivo, the source of radical production is not clear due to the nontarget specificity of DMPO and its analogs, so inhibition experiments of key enzymatic system may realistically work using cells. However, with tissues and in vivo, enzyme inhibition studies could be a challenge because inhibitors could become systemic especially in the latter.

REFERENCES

1. Sawyer DT, Valentine JS. How super is superoxide? *Acc Chem Res* 1981;**14**:393.
2. Buxton GV, Greenstock CL, Helman WP, Ross AB. Critical review of rate constants for reactions of hydrated electrons, hydrogen atoms and hydroxyl radicals (OH/O) in aqueous aolution. *J Phys Chem Ref* 1988;**17**:513.
3. Bagchi RN, Bond AM, Scholz F, Stoesser R. Characterization of the ESR spectrum of the superoxide anion in the liquid phase. *J Am Chem Soc* 1989;**111**:8270.
4. Nakanishi I, Ohkubo K, Fujita S, Fukuzumi S, Konishi T, Fujitsuka M, et al. Direct detection of superoxide anion generated in C60-photosensitized oxidation of NADH and an analogue by molecular oxygen. *J Chem Soc Perkin Trans* 2002;**2**:1829.
5. Petr A, Kataev V, Buechner B. First Direct In Situ EPR Spectroelectrochemical Evidence of the Superoxide Anion Radical. *J Phys Chem B* 2011;**115**:12036.
6. Symons MCR, Eastland GW, Denny LR. Effect of solvation on the electron spin resonance spectrum of the superoxide ion. *J Chem Soc Faraday Trans 1* 1980;**76**:1868.
7. Yu J, Chen J, Li C, Wang X, Zhang B, Ding H. ESR Signal of Superoxide Radical Anion Adsorbed on TiO2 Generated at Room Temperature. *J Phys Chem B* 2004;**108**:2781.
8. Bosnjakovic A, Schlick S. Nafion perfluorinated membranes treated in Fenton media: radical species detected by ESR spectroscopy. *J Phys Chem B* 2004;**108**:4332.
9. Mendiara SN, Ghibaudi E, Perissinotti LJ, Colussi AJ. Free radicals and diradicals in the reaction between nitrous acid and bisulfite in acid aqueous media. *J Phys Chem* 1992;**96**:8089.
10. Jiang J, Bank JF, Scholes CP. Subsecond time-resolved spin trapping followed by stopped-flow EPR of Fenton reaction products. *J Am Chem Soc* 1993;**115**:4742.
11. Weil JA, Bolton JR, Wertz JE. *Electron Paramagnetic Resonance: Elementary Theory and Practical Applications*. New York: John Wiley and Sons; 1994.
12. Klauschenz E, Haseloff RF, Volodarskii LB, Blasig IE. Spin Trapping Using 2,2-Dimethyl-2H-Imidazole-1-Oxides. *Free Radical Res* 1994;**20**:103.
13. Dikalov S, Kirilyuk I, Grigor'ev IA. Spin trapping of O-, C-, and S-centered radicals and peroxynitrite by 2H-imidazole-1-oxides. *Biochem Biophys Res Commun* 1996;**218**:616.
14. Bottle SE, Micallef AS. Synthesis and EPR spin trapping properties of a new isoindole-based nitrone: 1,1,3-trimethylisoindole N-oxide (TMINO). *Org Biomol Chem* 2003;**1**:2581.
15. Rosen GM, Tsai P, Barth ED, Dorey G, Casara P, Spedding M, et al. A one-step synthesis of 2-(2-Pyridyl)-3H-indol-3-one N-oxide: is it an efficient spin trap for hydroxyl radical? *J Org Chem* 2000;**65**:4460.
16. Khramtsov VV, Reznikov VA, Berliner LJ, Litkin AK, Grigor'ev IA, Clanton TL. NMR spin trapping: detection of free radical reactions with a new fluorinated DMPO analog. *Free Radical Biol Med* 2001;**30**:1099.
17. Thomas CE, Ohlweiler DF, Carr AA, Nieduzak TR, Hay DA, Adams G, et al. Characterization of the radical trapping activity of a novel series of cyclic nitrone spin traps. *J Biol Chem* 1996;**271**:3097.

18. Stolze K, Udilova N, Nohl H. ESR analysis of spin adducts of alkoxyl and lipid-derived radicals with the spin trap Trazon. *Biochem Pharmacol* 2002;**63**:1465.
19. Sankuratri N, Janzen EG. Synthesis and spin trapping chemistry of a novel bicyclic nitrone: 1,3,3-trimethyl-6-azabicyclo[3.2.1]oct-6-ene-N-oxide (Trazon). *Tetrahedron Lett* 1996;**37**:5313.
20. Durand G, Choteau F, Pucci B, Villamena FA. Reactivity of superoxide radical anion and hydroperoxyl radical with alpha-phenyl-N-tert-butylnitrone (PBN) derivatives. *J Phys Chem A* 2008;**112**:12498.
21. Frejaville C, Karoui H, Tuccio B, Le Moigne F, Culcasi M, Pietri S, et al. 5-(Diethoxyphosphoryl)-5-methyl-1-pyrroline N-oxide: a new efficient phosphorylated nitrone for the *in vitro* and *in vivo* spin trapping of oxygen-centered radicals. *J Med Chem* 1995;**38**:258.
22. Olive G, Mercier A, Moigne FL, Rockenbauer A, Tordo P. 2-ethoxycarbonyl-2-methyl-3,4-dihydro-2H-pyrrole-1-oxide: evaluation of the spin trapping properties. *Free Radical Biol Med* 2000;**28**:403.
23. Villamena FA, Rockenbauer A, Gallucci J, Velayutham M, Hadad CM, Zweier JL. Spin trapping by 5-carbamoyl-5-methyl-1-pyrroline N-oxide (AMPO): theoretical and experimental studies. *J Org Chem* 2004;**69**:7994.
24. Villamena FA, Xia S, Merle JK, Lauricella R, Tuccio B, Hadad CM, et al. Reactivity of Superoxide Radical Anion with Cyclic Nitrones: Role of Intramolecular H-Bond and Electrostatic Effects. *J Am Chem Soc* 2007;**129**:8177.
25. Buettner GR. On the reaction of superoxide with DMPO/.OOH. *Free Radic Res Commun* 1990;**10**:11.
26. Allouch A, Lauricella RP, Tuccio BN. Effect of pH on superoxide/hydroperoxyl radical trapping by nitrones: an EPR/kinetic study. *Mol Phys* 2007;**105**:2017.
27. Pou S, Ramos CL, Gladwell T, Renks E, Centra M, Young D, et al. A Kinetic Approach to the Selection of a Sensitive Spin Trapping System for the Detection of Hydroxyl Radical. *Analytical Biochemistry* 1994;**217**:76.
28. Davies MJ, Forni LG, Shuter SL. Electron spin resonance and pulse radiolysis studies on the spin trapping of sulphur-centered radicals. *Chem-Biol Interact* 1987;**61**:177.
29. Villamena FA, Hadad CM, Zweier JL. Kinetic Study and Theoretical Analysis of Hydroxyl Radical Trapping and Spin Adduct Decay of Alkoxycarbonyl and Dialkoxyphosphoryl Nitrones in Aqueous Media. *J Phys Chem A* 2003;**107**:4407.
30. Buettner GR. The pecking order of free radicals and antioxidants: lipid peroxidation, alpha-tocopherol, and ascorbate. *Arch Biochem Biophys* 1993;**300**:535.
31. Madej E, Wardman P. The oxidizing power of the glutathione thiyl radical as measured by its electrode potential at physiological pH. *Arch Biochem Biophys* 2007;**462**:94.
32. Villamena FA, Merle JK, Hadad CM, Zweier JL. Superoxide Radical Anion Adduct of 5,5-Dimethyl-1-pyrroline N-Oxide (DMPO). 2. The Thermodynamics of Decay and EPR Spectral Properties. *J Phys Chem A* 2005;**109**:6089.
33. Behar D, Czapski G, Rabani J, Dorfman LM, Schwarz HA. Acid dissociation constant and decay kinetics of the perhydroxyl radical. *J Phys Chem* 1970;**74**:3209.
34. Czapski G, Bielski BHJ. The formation and decay of H_2O_3 and HO_2 in electron-irradiated aqueous solutions. *J Phys Chem* 1963;**67**:2180.
35. Villamena FA, Merle JK, Hadad CM, Zweier JL. Superoxide radical anion adduct of 5,5-dimethyl-1-pyrroline n-oxide (DMPO). 1. The thermodynamics of formation and its acidity. *J Phys Chem A* 2005;**109**:6083.
36. Burgett RA, Bao X, Villamena FA. Superoxide radical anion adduct of 5,5-dimethyl-1-pyrroline N-oxide (DMPO). 3. Effect of mildly acidic pH on the thermodynamics and kinetics of adduct formation. *J Phys Chem A* 2008;**112**:2447.
37. Finkelstein E, Rosen GM, Rauckman EJ. Spin trapping. Kinetics of the reaction of superoxide and hydroxyl radicals with nitrones. *J Am Chem Soc* 1980;**102**:4994.
38. Villamena FA, Zweier JL. Superoxide radical trapping and spin adduct decay of 5-tert-butoxycarbonyl-5-methyl-1-pyrroline N-oxide (BocMPO): kinetics and theoretical analysis. *J Chem Soc Perkin Trans* 2002;**2**:1340.

39. Frejaville C, Karoui H, Tuccio B, Le Moigne F, Culcasi M, Pietri S, et al. 5-(Diethoxyphosphoryl)-5-methyl-1-pyrroline N-oxide: a new phosphorylated nitrone for the efficient in vitro and in vivo spin trapping of oxygen-centered radicals. *J Chem Soc Chem Commun* 1994;1793.
40. Allouch A, Roubaud V, Lauricella R, Bouteiller J-C, Tuccio B. Spin trapping of superoxide by diester-nitrones. *Org Biomol Chem* 2005;**3**:2458.
41. Lauricella R, Allouch A, Roubaud V, Bouteiller J-C, Tuccio B. A new kinetic approach to the evaluation of rate constants for the spin trapping of superoxide/hydroperoxyl radical by nitrones in aqueous media. *Org Biomol Chem* 2004;**2**:1304.
42. Lauricella RP, Bouteiller J-CH, Tuccio BN. Evidence of overestimation of rate constants for the superoxide trapping by nitrones in aqueous media. *Phys Chem Chem Phys* 2005;**7**:399.
43. Tsai P, Ichikawa K, Mailer C, Pou S, Halpern HJ, Robinson BH, et al. Esters of 5-carboxyl-5-methyl-1-pyrroline N-oxide: A family of spin traps for superoxide. *J Org Chem* 2003;**68**:7811.
44. Kezler A, Kalyanaraman B, Hogg N. Comparative investigation of superoxide radical trapping by cyclic nitrone spin traps. *Free Radical Biol Med* 2003;**35**:1149.
45. Goldstein S, Rosen GM, Russo A, Samuni A. Kinetics of spin trapping superoxide, hydroxyl, and aliphatic radicals by cyclic nitrones. *J Phys Chem A* 2004;**108**:6679.
46. Yamazaki I, Piette LH, Grover TA. Kinetic studies on spin trapping of superoxide and hydroxyl radicals generated in NADPH-cytochrome P-450 reductase-paraquat systems. Effect of iron chelates. *J Biol Chem* 1990;**265**:652.
47. Han Y, Tuccio B, Lauricella R, Villamena FA. Improved Spin Trapping Properties by beta-Cyclodextrin-Cyclic Nitrone Conjugate. *J Org Chem* 2008;**73**:7108.
48. Kim S-U, Liu Y, Nash KM, Zweier JL, Rockenbauer A, Villamena FA. Fast Reactivity of Cyclic Nitrone-Calix[4]pyrrole Conjugate with Superoxide Radical Anion: Theoretical and Experimental Studies. *J Am Chem Soc* 2010;**132**:17157.
49. Chalier F, Tordo P. 5-Diisopropoxyphosphoryl-5-methyl-1-pyrroline N-oxide, DIPPMPO, a crystalline analog of the nitrone DEPMPO: synthesis and spin trapping properties. *J Chem Soc Perkin Trans* 2002;**2**:2110.
50. Buettner GR, Oberley LW. Considerations in the spin trapping of superoxide and hydroxyl radical in aqueous systems using 5,5-dimethyl-1-pyrroline-1-oxide. *Biochem Biophys Res Commun* 1978;**83**:69.
51. Burkitt MJ, Tsang SY, Tam SC, Bremner I. Generation of 5,5-dimethyl-1-pyrroline N-oxide hydroxyl and scavenger radical adducts from copper/H2O2 mixtures: effects of metal ion chelation and the search for high-valent metal-oxygen intermediates. *Arch Biochem Biophys* 1995;**323**:63.
52. Villamena FA. Superoxide Radical Anion Adduct of 5,5-Dimethyl-1-pyrroline N-Oxide. 5. Thermodynamics and Kinetics of Unimolecular Decomposition. *J Phys Chem A* 2009;**113**:6398.
53. Villamena FA. Superoxide Radical Anion Adduct of 5,5-Dimethyl-1-pyrroline N-Oxide. 6. Redox Properties. *J Phys Chem A* 2009;**114**:1153.
54. Khan N, Wilmot CM, Rosen GM, Demidenko E, Sun J, Joseph J, et al. Spin traps: in vitro toxicity and stability of radical adducts. *Free Radic Biol Med* 2003;**34**:1473.
55. Karoui H, Rockenbauer A, Pietri S, Tordo P. Spin trapping of superoxide in the presence of beta-cyclodextrins. *Chem Commun (Cambridge, UK)* 2002;3030.
56. Bardelang D, Rockenbauer A, Karoui H, Finet J-P, Biskupska I, Banaszak K, et al. Inclusion complexes of EMPO derivatives with 2,6-di-O-methyl-beta-cyclodextrin: synthesis, NMR and EPR investigations for enhanced superoxide detection. *Org Biomol Chem* 2006;**4**:2874.
57. Zweier JL, Broderick R, Kuppusamy P, Thompson-Gorman S, Lutty GA. Determination of the mechanism of free radical generation in human aortic endothelial cells exposed to anoxia and reoxygenation. *J Biol Chem* 1994;**269**:24156.
58. Xia Y, Zweier JL. Superoxide and peroxynitrite generation from inducible nitric oxide synthase in macrophages. *Proc Natl Acad Sci USA* 1997;**94**:6954.
59. Snyrychova I. Improvement of the sensitivity of EPR spin trapping in biological systems by cyclodextrins: A model study with thylakoids and photosystem II particles. *Free Radic Biol Med* 2010;**48**:264.
60. Das A, Gopalakrishnan B, Druhan LJ, Wang TY, De Pascali F, Rockenbauer A, et al. Reversal of SIN-1-induced eNOS dysfunction by the spin trap, DMPO, in bovine aortic endothelial cells via eNOS phosphorylation. *Br J Pharmacol* 2014;**171**:2321.

61. Hardy M, Bardelang D, Karoui H, Rockenbauer A, Finet J-P, Jicsinszky L, et al. Improving the Trapping of Superoxide Radical with a Beta-Cyclodextrin- 5-Diethoxyphosphoryl-5-methyl-1-pyrroline-N-oxide (DEPMPO) Conjugate. *Chem - Eur J* 2009;**15**:11114.
62. Beziere N, Hardy M, Poulhes F, Karoui H, Tordo P, Ouari O, et al. Metabolic stability of superoxide adducts derived from newly developed cyclic nitrone spin traps. *Free Radical Biol Med* 2014;**67**:150.
63. McIntire GL, Blount HN, Stronks HJ, Shetty RV, Janzen EG. Spin trapping in electrochemistry. 2. Aqueous and nonaqueous electrochemical characterizations of spin traps. *J Phys Chem* 1980;**84**:916.
64. Koppenol WH. Thermodynamics of reactions involving nitrogen-oxygen compounds. *Methods Enzymol* 1996;**268**:7.
65. Haseloff RF, Mertsch K, Rohde E, Baeger I, Grigor'ev IA, Blasig IE. Cytotoxicity of spin trapping compounds. *FEBS Lett* 1997;**418**:73.
66. Rohr-Udilova N, Stolze K, Marian B, Nohl H. Cytotoxicity of novel derivatives of the spin trap EMPO. *Bioorg Med Chem Lett* 2006;**16**:541.
67. Durand G, Prosak RA, Han Y, Ortial S, Rockenbauer A, Pucci B, et al. Spin trapping and cytoprotective properties of fluorinated amphiphilic carrier conjugates of cyclic versus linear nitrones. *Chem Res Toxicol* 2009;**22**:1570.
68. Janzen EG, Poyer JL, Schaefer CF, Downs PE, DuBose CM. Biological spin trapping. II. Toxicity of nitrone spin traps: dose-ranging in the rat. *J Biochem Biophys Methods* 1995;**30**:239.
69. Schaefer CF, Janzen EG, West MS, Poyer JL, Kosanke SD. Blood chemistry changes in the rat induced by high doses of nitronyl free radical spin traps. *Free Radic Biol Med* 1996;**21**:427.
70. Liu K, Jiang J, Ji L, Shi X, Swartz H. An HPLC and EPR investigation on the stability of DMPO and DMPO spin adducts in vivo. *Res Chem Intermed* 1996;**22**:499.
71. Breuer E, Aurich HG, Nielsen A. *Nitrones, Nitronates and Nitroxides*. New York: John Wiley and Sons; 1989.
72. Torsell KBG. *Nitrile Oxides, Nitrones, and Nitronates in Organic Synthesis*. VCH Verlagsgesellschaft mbH: Weinheim; 1988.
73. Murahashi SI. Synthetic apects of metal-catalyzed oxidations of amines and related reactions. *Angew Chem Int Ed Engl* 1995;**34**:2443.
74. Rosen GM, Britigan BE, Halpern HJ, Pou S. *Free Radicals: Biology and Detection by Spin Trapping*. New York: Oxford University Press; 1999.
75. Villamena FA, Dickman MH, Crist DR. Nitrones as Ligands in Complexes of Cu(II), Mn(II), Co (II), Ni(II), Fe(II), and Fe(III) with N-tert-Butyl–(2-pyridyl)nitrone and 2,5,5-Trimethyl-1-pyrroline-N-oxide. *Inorg Chem* 1998;**37**:1446.
76. Zhang Y-K, Lu D-H, Xu GZ. Synthesis and radical additional sterochemistry of two trimethyl-1-pyrroline 1-oxides as studied by EPR spectroscopy. *J Chem Soc Perkin Trans* 1991;**2**:1855–60.
77. Turner MJ, Rosen GM. Spin trapping of superoxide and hydroxyl radicals with substituted pyrroline 1-oxides. *J Med Chem* 1986;**29**:2439.
78. Villamena F, Zweier J. Superoxide radical trapping and spin adduct decay of 5-tert-butoxycarbonyl-5-methyl-1-pyrroline N-oxide (BocMPO): kinetics and theoretical analysis. *J Chem Soc Perkin Trans* 2002;**2**:1340.
79. Pou S, Rosen GM, Wu Y, Rosen GM. Synthesis of deuterium and ^{15}N-containing pyrroline 1-oxides: Spin trapping study. *J Org Chem* 1990;**55**:4438.
80. Cisneros L, Serna P, Corma A. Selective reductive coupling of nitro compounds with aldehydes to nitrones in H2 using carbon-supported and -decorated platinum nanoparticles. *Angew Chem Int Ed* 2014;**53**:9306.
81. Joseph R, Sudalai A, Ravindranathan T. Catalytic oxidation of secondary amines with H_2O_2 over molecular sieves: A high yield and single step preparation. *Synlett* 1995;1177.
82. Murahashi SI, Mitsui H, Shiota T, Tsuda T, Watanabe S. Tungstate-catalyzed oxidation of secondary amines to nitrones. a-Substitution of secondary amines via nitrones. *J Org Chem* 1990;**55**:1736.
83. Murahashi SI, Shiota T. Selenium dioxide catalyzed oxidation of secondary amines with hydrogen peroxide. Simple synthesis of nitrones from secondary amines. *Tetrahedron Lett* 1987;**28**:2383.
84. Forcato M, Nugent WA, Licini G. A "waterproof" catalyst for the oxidation of secondary amines to nitrones with alkyl hydroperoxides. *Tetrahedron Lett* 2003;**44**:49.
85. Tokuyama H, Kuboyama T, Amano A, Yamashita T, Fukuyama T. A novel transformation of primary amines to N-monoalkylhydroxylamines. *Synthesis* 2000;1299.

86. Boyd DR, Coulter PB, McGuckin MR, Sharma ND, Jennings WB, Wilson VE. Imines and derivatives. Part 24. Nitrone synthesis by imine oxidation using either a peroxyacid or dimethyldioxirane. *J Chem Soc Perkin Trans* 1990;**1**:301.
87. Ferrer M, Sanchez-Baeza F, Casas J, Messeguer A. Decomposition of dioxiranes induced by dialkyl ethers. *Tetrahedron Lett* 1994;**35**:2981.
88. Busque F, de March P, Figueredo M, Font J, Gallagher T, Milan S. Efficient synthesis of (S)-3,4-dihydro-2-[(pivaloyloxy)methyl]-2H-pyrrole 1-oxide. *Tetrahedron: Asymmetry* 2002;**13**:437.
89. Dehnel A, Griller D, Kanabus-Kaminska JM. Designer spin traps with a cyclic nitrone structure. *J Org Chem* 1988;**53**:1566.
90. Cicchi S, Corsi M, Goti A. Inexpensive and environmentally friendly oxidation of hydroxylamine to nitrones with bleach. *J Org Chem* 1999;**64**:7243.
91. Cicchi S, Marradi M, Goti A, Brandi A. Manganese dioxide oxidation of hydroxylamines to nitrones. *Tetrahedron Lett* 2001;**42**:6503.
92. Zauche TH, Espenson JH. Kinetics and mechanism of the oxidation of secondary hydroxylamines to nitrones with hydrogen peroxide, catalyzed by methylrhenium trioxide. *Inorg Chem* 1997;**36**:5257.
93. Bonnett R, Brown RFC, Clark VM, Sutherland IO, Todd A. Experiments towards the synthesis of corrins. Part II. The preparation and reactions of D^1-pyrroline 1-oxides. *J Chem Soc* 1959;2094.
94. Buehler E. Alkylation of syn- and anti-benzaldoximes. *J Org Chem* 1967;**32**:261.
95. Christensen D, Jorgensen KA, Hazell RG. Rearrangement reactions of oxaziridines to nitrones. X-Ray crystal and molecular structure of N-t-butyl-[small alpha](o-hydroxyphenyl)nitrone. *J Chem Soc Perkin Trans* 1990;**1**:2391.
96. Griffith OH, Cornell DW, McConnell HM. Nitrogen hyperfine tensor and g tensor of nitroxide radicals. *J Chem Phys* 1965;**43**:2909.
97. Taniguchi H, Madden KP. DMPO-alkyl radical spin trapping: an in situ radiolysis steady-state ESR study. *Radiat Res* 2000;**153**:447.
98. Taniguchi H, Madden KP. In Situ Radiolysis Steady-State ESR Study of Carboxyalkyl Radical Trapping by 5,5-Dimethyl-1-pyrroline-N-oxide: Spin Adduct Structure and Stability. *J Phys Chem A* 1998;**102**:6753.
99. Cholvad V, Szaboova K, Stasko A, Nuyken O, Voit B. ESR parameters of 5,5-dimethylpyrrolidine 1-oxide (DMPO) spin adducts in the photochemical decomposition of azo compounds. *Magn Reson Chem* 1991;**29**:402.
100. Davies MJ, Forni LG, Shuter SL. Electron spin resonance and pulse radiolysis studies on the spin trapping of sulfur-centered radicals. *Chem-Biol Interact* 1987;**61**:177.
101. Villamena FA, Locigno EJ, Rockenbauer A, Hadad CM, Zweier JL. Theoretical and experimental studies of the spin trapping of inorganic radicals by 5,5-dimethyl-1-pyrroline N-oxide (DMPO). 1. Carbon dioxide radical anion. *J Phys Chem A* 2006;**110**:13253.
102. Villamena FA, Locigno EJ, Rockenbauer A, Hadad CM, Zweier JL. Theoretical and experimental studies of the spin trapping of inorganic radicals by 5,5-dimethyl-1-pyrroline N-oxide (DMPO). 2. Carbonate radical anion. *J Phys Chem A* 2007;**111**:384.
103. Nash KM, Rockenbauer A, Villamena FA. Reactive nitrogen species reactivities with nitrones: theoretical and experimental studies. *Chem Res Toxicol* 2012;**25**:1581.
104. Zamora PL, Villamena FA. Theoretical and Experimental Studies of the Spin Trapping of Inorganic Radicals by 5,5-Dimethyl-1-pyrroline N-Oxide (DMPO). 3. Sulfur Dioxide, Sulfite, and Sulfate Radical Anions. *J Phys Chem A* 2012;**116**:7210.
105. Reszka K, Bilski P, Chignell CF. EPR spectra of DMPO spin adducts of superoxide and hydroxyl radicals in pyridine. *Free Rad Res Commun* 1992;**17**:377.
106. Josephy PD, Rehorek D, Janzen EG. Electron spin resonance spin trapping of thiyl, radicals from the decomposition of thionitrites. *Tetrahedron Lett* 1984;**25**:1685.
107. Bradshaw TP, McMillan DC, Crouch RK, Jollow DJ. Identification of free radicals produced in rat erythrocytes exposed to hemolytic concentrations of phenylhydroxylamine. *Free Radic Biol Med* 1995;**18**:279.

108. Villamena FA, Liu Y, Zweier JL. Superoxide radical anion adduct of 5,5-dimethyl-1-pyrroline N-oxide. 4. Conformational effects on the EPR hyperfine splitting constants. *J Phys Chem A* 2008;**112**:12607.
109. Clement JL, Ferre N, Siri D, Karoui H, Rockenbauer A, Tordo P. Assignment of the EPR spectrum of 5,5-dimethyl-1-pyrroline N-oxide (DMPO) superoxide spin adduct. *J Org Chem* 2005;**70**:1198.
110. Rosen GM, Beselman A, Tsai P, Pou S, Mailer C, Ichikawa K, et al. Influence of conformation on the EPR spectrum of 5,5-dimethyl-1-hydroperoxy-1-pyrrolidinyloxyl: a spin trapped adduct of superoxide. *J Org Chem* 2004;**69**:1321.
111. Villamena FA, Hadad CM, Zweier JL. Theoretical study of the spin trapping of hydroxyl radical by cyclic nitrones: a density functional theory approach. *J Am Chem Soc* 2004;**126**:1816.
112. Karoui H, Chalier F, Finet J-P, Tordo P. DEPMPO: an efficient tool for the coupled ESR-spin trapping of alkylperoxyl radicals in water. *Org Biomol Chem* 2011;**9**:2473.
113. Villamena FA, Zweier JL. Detection of reactive oxygen and nitrogen species by EPR spin trapping. *Antioxid Redox Signal* 2004;**6**:619.
114. Duling DR. Simulation of Multiple Isotropic Spin-Trap EPR Spectra. *Journal of Magnetic Resonance Series B* 1994;**104**:105.
115. Stoll S, Schweiger A. EasySpin, a comprehensive software package for spectral simulation and analysis in EPR. *J Magn Reson* 2006;**178**:42.
116. Rockenbauer A, Korecz L. Automatic Computer Simulations of ESR Spectra. *Appl Magn Reson* 1996;**10**:29.
117. Samouilov A, Roubaud V, Kuppusamy P, Zweier JL. Kinetic analysis-based quantitation of free radical generation in EPR spin trapping. *Analytical Biochemistry* 2004;**334**:145.
118. Hanna PM, Chamulitrat W, Mason RP. When are metal ion-dependent hydroxyl and alkoxyl radical adducts of 5,5-dimethyl-1-pyrroline N-oxide artifacts? *Arch Biochem Biophys* 1992;**296**:640.
119. Eberson L. *Toxicology of the Human Environment: The Critical Role of Free Radicals*. New York, NY: Taylor and Francis, Inc; 2000.
120. Kanabus-Kaminska JM, Gilbert BC, Griller D. Solvent effects on the thermochemistry of free-radical reactions. *J Am Chem Soc* 1989;**111**:3311.
121. Mason R, Kadiiska M. In: Eaton S, Eaton G, Berliner L, editors. *Biomedical EPR, Part A: Free Radicals, Metals, Medicine, and Physiology*, Vol. 23. US: Springer; 2005. p. 93.
122. Zweier JL, Kuppusamy P, Thompson-Gorman S, Klunk D, Lutty GA. Measurement and characterization of free radical generation in reoxygenated human endothelial cells. *Am J Physiol* 1994;**266**: C700.
123. Shi H, Timmins G, Monske M, Burdick A, Kalyanaraman B, Liu Y, et al. Evaluation of spin trapping agents and trapping conditions for detection of cell-generated reactive oxygen species. *Arch Biochem Biophys* 2005;**437**:59.
124. Hougaard AB, Arneborg N, Andersen ML, Skibsted LH. ESR spin trapping for characterization of radical formation in Lactobacillus acidophilus NCFM and Listeria innocua. *J Microbiol Methods* 2013;**94**:205.
125. Ranguelova K, Rice AB, Khajo A, Triquigneaux M, Garantziotis S, Magliozzo RS, et al. Formation of reactive sulfite-derived free radicals by the activation of human neutrophils: an ESR study. *Free Radic Biol Med* 2012;**52**:1264.
126. Deschacht M, Horemans T, Martinet W, Bult H, Maes L, Cos P. Comparative EPR study of different macrophage types stimulated for superoxide and nitric oxide production. *Free Radic Res* 2010;**44**:763.
127. Bannister JV, Bannister WH. Production of oxygen-centered radicals by neutrophils and macrophages as studied by electron spin resonance (ESR). *Environ Health Perspect* 1985;**64**:37.
128. Dikalov SI, Mason RP. Spin trapping of polyunsaturated fatty acid-derived peroxyl radicals: reassignment to alkoxyl radical adducts. *Free Radic Biol Med* 2001;**30**:187.
129. Zhao B, He Y-Y, Bilski PJ, Chignell CF. Pristine (C60) and Hydroxylated [C60(OH)24] Fullerene Phototoxicity towards HaCaT Keratinocytes: Type I vs Type II Mechanisms. *Chem Res Toxicol* 2008;**21**:1056.

130. Sugimoto R, Kumagai Y, Nakai Y, Ishii T. 9,10-Phenanthraquinone in diesel exhaust particles downregulates Cu,Zn-SOD and HO-1 in human pulmonary epithelial cells: Intracellular iron scavenger 1,10-phenanthroline affords protection against apoptosis. *Free Radical Biol Med* 2005;**38**:388.
131. Rota C, Fann YC, Mason RP. Phenoxyl free radical formation during the oxidation of the fluorescent dye 2',7'-dichlorofluorescein by horseradish peroxidase. Possible consequences for oxidative stress measurements. *J Biol Chem* 1999;**274**:28161.
132. Chen C, Zhou B, Lu D, Xu G. Electron transfer events in solutions of cyanine dyes. *J Photochem Photobiol A* 1995;**89**:25.
133. Masaki H, Okano Y, Sakurai H. Generation of active oxygen species from advanced glycation end-products (AGEs) during ultraviolet light A (UVA) irradiation and a possible mechanism for cell damaging. *Biochim Biophys Acta Gen Subj* 1999;**1428**:45.
134. Zang L-y, Stone K, Pryor WA. Detection of free radicals in aqueous extracts of cigarette tar by electron spin resonance. *Free Radical Biol Med* 1995;**19**:161.
135. Chignell CF, Bilski P, Reszka KJ, Motten AG, Sik RH, Dahl TA. Spectral and photochemical properties of curcumin. *Photochem Photobiol* 1994;**59**:295.
136. Xia Y, Tsai A-L, Berka V, Zweier JL. Superoxide generation from endothelial nitric-oxide synthase. A Ca2 + /calmodulin-dependent and tetrahydrobiopterin regulatory process. *J Biol Chem* 1998;**273**:25804.
137. Vasquez-Vivar J, Martasek P, Hogg N, Karoui H, Masters BSS, Pritchard KA, et al. Electron spin resonance spin-trapping detection of superoxide generated by neuronal nitric oxide synthase. *Methods Enzymol* 1999;**301**:169.
138. Xia Y, Berlowitz CO, Zweier JL. PIN inhibits nitric oxide and superoxide production from purified neuronal nitric oxide synthase. *Biochim Biophys Acta, Gen Subj* 2006;**1760**:1445.
139. Cardounel AJ, Xia Y, Zweier JL. Endogenous Methylarginines Modulate Superoxide as Well as Nitric Oxide Generation from Neuronal Nitric-oxide Synthase: Differences in the Effects of Monomethyl- and Dimethylarginines in the Presence and Absence of Tetrahydrobiopterin. *J Biol Chem* 2005;**280**:7540.
140. Xia Y, Roman LJ, Masters BSS, Zweier JL. Inducible nitric-oxide synthase generates superoxide from the reductase domain. *J Biol Chem* 1998;**273**:22635.
141. Xia Y, Zweier JL. Superoxide and peroxynitrite generation from inducible nitric oxide synthase in macrophages. *Proc Natl Acad Sci USA* 1997;**94**:6954.
142. Chamulitrat W, Hughes MF, Eling TE, Mason RP. Superoxide and peroxyl radical generation from the reduction of polyunsaturated fatty acid hydroperoxides by soybean lipoxygenase. *Arch Biochem Biophys* 1991;**290**:153.
143. Kukavica B, Mojovic M, Vuccinic Z, Maksimovic V, Takahama U, Jovanovic SV. Generation of hydroxyl radical in isolated pea root cell wall, and the role of cell wall-bound peroxidase, Mn-SOD and phenolics in their production. *Plant Cell Physiol* 2009;**50**:304.
144. Kundu TK, Velayutham M, Zweier JL. Aldehyde Oxidase Functions as a Superoxide Generating NADH Oxidase: An Important Redox Regulated Pathway of Cellular Oxygen Radical Formation. *Biochemistry* 2012;**51**:2930.
145. Velayutham M, Hemann C, Zweier JL. Removal of H2O2 and generation of superoxide radical: Role of cytochrome c and NADH. *Free Radical Biol Med* 2011;**51**:160.
146. Chen J, Chen C-L, Rawale S, Chen C-A, Zweier JL, Kaumaya PTP, et al. Peptide-based Antibodies against Glutathione-binding Domains Suppress Superoxide Production Mediated by Mitochondrial Complex I. *J Biol Chem* 2010;**285**:3168.
147. Chen Y-R, Chen C-L, Yeh A, Liu X, Zweier JL. Direct and Indirect Roles of Cytochrome b in the Mediation of Superoxide Generation and NO Catabolism by Mitochondrial Succinate-Cytochrome c Reductase. *J Biol Chem* 2006;**281**:13159.
148. Chen Y-R, Chen C-L, Zhang L, Green-Church KB, Zweier JL. Superoxide Generation from Mitochondrial NADH Dehydrogenase Induces Self-inactivation with Specific Protein Radical Formation. *J Biol Chem* 2005;**280**:37339.

149. Hardy M, Chalier F, Ouari O, Finet J-P, Rockenbauer A, Kalyanaraman B, et al. Mito-DEPMPO synthesized from a novel NH2-reactive DEPMPO spin trap: a new and improved trap for the detection of superoxide. *Chem Commun (Cambridge, UK)* 2007;1083.
150. Morehouse KM, Moreno SNJ, Mason RP. The one-electron reduction of uroporphyrin I by rat hepatic microsomes. *Arch Biochem Biophys* 1987;**257**:276.
151. Harbour JR, Bolton JR. Superoxide formation in spinach chloroplasts: Electron spin resonance detection by spin trapping. *Biochem Biophys Res Commun* 1975;**64**:803.
152. Gopalakrishnan B, Nash KM, Velayutham M, Villamena FA. Detection of nitric oxide and superoxide radical anion by electron paramagnetic resonance spectroscopy from cells using spin traps. *J Visualized Exp* 2012. E2810/1.
153. Shi H, Timmins G, Monske M, Burdick A, Kalyanaraman B, Liu Y, et al. Evaluation of spin trapping agents and trapping conditions for detection of cell-generated reactive oxygen species. *Arch Biochem Biophys* 2005;**437**:59.
154. Sankarapandi S, Zweier JL, Mukherjee G, Quinn MT, Huso DL. Measurement and characterization of superoxide generation in microglial cells: evidence for an NADPH oxidase-dependent pathway. *Arch Biochem Biophys* 1998;**353**:312.
155. Silverton SF, Mesaros S, Markham GD, Malinski T. Osteoclast radical interactions: NADPH causes pulsatile release of NO and stimulates superoxide production. *Endocrinology* 1995;**136**:5244.
156. Zweier JL, Duke SS, Kuppusamy P, Sylvester JT, Gabrielson EW. Electron paramagnetic resonance evidence that cellular oxygen toxicity is caused by the generation of superoxide and hydroxyl free radicals. *FEBS Lett* 1989;**252**:12.
157. Zweier JL, Kuppusamy P, Lutty GA. Measurement of endothelial cell free radical generation: evidence for a central mechanism of free radical injury in postischemic tissues. *Proc Natl Acad Sci USA* 1988;**85**:4046.
158. Togashi H, Shinzawa H, Matsuo T, Takeda Y, Takahashi T, Aoyama M, et al. Analysis of hepatic oxidative stress status by electron spin resonance spectroscopy and imaging. *Free Radical Biol Med* 2000;**28**:846.
159. Zweier JL. Measurement of superoxide-derived free radicals in the reperfused heart. Evidence for a free radical mechanism of reperfusion injury. *J Biol Chem* 1988;**263**:1353.
160. Zweier JL, Kuppusamy P, Williams R, Rayburn BK, Smith D, Weisfeldt ML, et al. Measurement and characterization of postischemic free radical generation in the isolated perfused heart. *J Biol Chem* 1989;**264**:18890.
161. Haywood R, Andrady C, Kassouf N, Sheppard N. Intensity-dependent direct solar radiation- and UVA-induced radical damage to human skin and DNA, lipids and proteins. *Photochem Photobiol* 2011;**87**:117.
162. Souza HP, Souza LC, Anastacio VM, Pereira AC, Junqueira ML, Krieger JE, et al. Vascular oxidant stress early after balloon injury: evidence for increased NAD(P)H oxidoreductase activity. *Free Radic Biol Med* 2000;**28**:1232.
163. Hartell MG, Borzone G, Clanton TL, Berliner LJ. Detection of free radicals in blood by electron spin resonance in a model of respiratory failure in the rat. *Free Radic Biol Med* 1994;**17**:467.
164. Kadiiska MB, Mason RP. Ethylene glycol generates free radical metabolites in rats: an ESR in vivo spin trapping investigation. *Chem Res Toxicol* 2000;**13**:1187.
165. Ghio AJ, Kadiiska MB, Xiang QH, Mason RP. In vivo evidence of free radical formation after asbestos instillation: an ESR spin trapping investigation. *Free Radic Biol Med* 1998;**24**:11.
166. Mergner GW, Weglicki WB, Kramer JH. Postischemic free radical production in the venous blood of the regionally ischemic swine heart. Effect of deferoxamine. *Circulation* 1991;**84**:2079.
167. Lai EK, Crossley C, Sridhar R, Misra HP, Janzen EG, McCay PB. In vivo spin trapping of free radicals generated in brain, spleen, and liver during gamma radiation of mice. *Arch Biochem Biophys* 1986;**244**:156.
168. Murray AR, Kisin E, Castranova V, Kommineni C, Gunther MR, Shvedova AA. Phenol-induced in vivo oxidative stress in skin: evidence for enhanced free radical generation, thiol oxidation, and antioxidant depletion. *Chem Res Toxicol* 2007;**20**:1769.